C. 1

DOWEL ACTION
IN
REINFORCED CONCRETE CONSTRUCTION
(BEAM-COLUMN CONNECTIONS)

by

ELY E. KAZAKOFF

B.A.Sc., University of British Columbia, 1971

A THESIS SUBMITTED IN PARTIAL FULFILMENT OF

THE REQUIREMENTS FOR THE DEGREE OF

MASTER OF APPLIED SCIENCE

In the Department

of

CIVIL ENGINEERING

We accept this thesis as conforming to the required standard

THE UNIVERSITY OF BRITISH COLUMBIA

April 1974

In presenting this thesis in partial fulfilment of the requirements for an advanced degree at the University of British Columbia, I agree that the Library shall make it freely available for reference and study. I further agree that permission for extensive copying of this thesis for scholarly purposes may be granted by the Head of my Department or by his representatives. It is understood that copying or publication of this thesis for financial gain shall not be allowed without my written permission.

Ely E. Kazakoff

Department of CIVIL ENGINEERING
The University of British Columbia
Vancouver 8, Canada

April 1974

ABSTRACT

The transfer of shear in a beam-column joint by dowel action alone was experimentally and analytically studied. The laboratory work involved the shear capacity determination of individual reinforcing steel dowels embedded in concrete. Two main series of experimental tests were conducted on bottom and top dowels - component parts of a beam-column joint. All experimental results were compared to a theoretical analysis.

The theoretical analysis consisted of choosing a rational physical model, i.e., a mode of behaviour for each of the two component parts of the joint. No curve-fitting to the experimental results was done. These results do show, however, that the model provides a safe lower bound on the shear capacity of the joint. Also, the model permits reasonable extrapolation to other design problems where the conditions of the problem are not exactly the same as those imposed during the experimental tests.

A design example of predicting the shear capacity of a beam-column joint on the basis of dowel action of the reinforcing steel is presented for any combination of top and bottom dowels.

TABLE OF CONTENTS

LIST OF FIGURES

LIST OF TABLES

ACKNOWLEDGEMENTS

I wish to express my appreciation to Professor S. L. Lipson for his guidance and help throughout this thesis. Also, I wish to thank Messrs. R. Postgate, B. Merkli, W. Schmitt, and J. Sharpe for their assistance in making the test equipment and carrying out the tests. Finally, I wish to acknowledge financial assistance from the National Research Council of Canada and the Computer Centre of the University of British Columbia.

April 1974

Vancouver, B. C.

CHAPTER 1. INTRODUCTION

In order to determine the shear capacity of a reinforced concrete beam-column joint, where all the shear is transferred solely by dowel action of the reinforcing steel bars crossing the beam-column interface, an experimental test program was conducted and the results compared with a theoretical analysis. This type of joint could be made by forming and pouring a cast-in-place beam against a precast column which already has the necessary bottom and top dowels protruding from it. The reverse case is also possible. A precast beam with bottom and top dowels protruding from its end could be positioned against a formed column and the column subsequently cast-in-place. The effect of frictional shear between the beam-column interface has not been considered in this investigation. Only the dowel action of the steel bars is considered.

The beam-column joint as shown in Fig. 1.1a can be broken down into its component parts - bottom and top dowels (Fig. 1.1b and 1.1c).

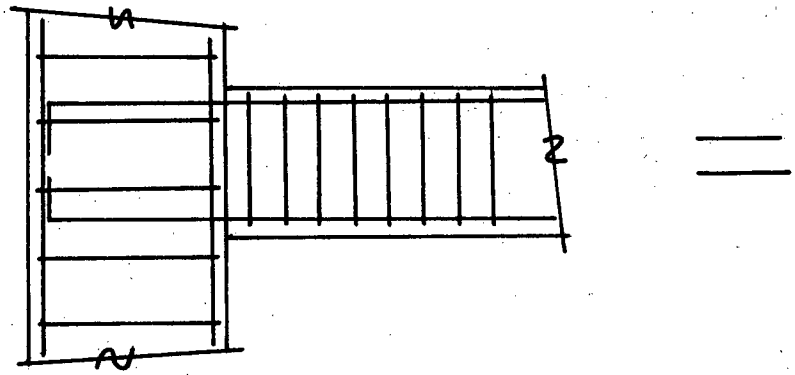

Fig. 1.1a Beam-Column Joint

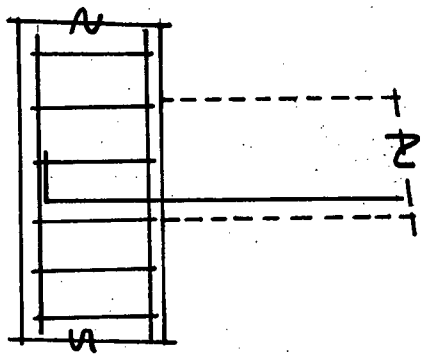

Fig. 1.1b Bottom Dowel

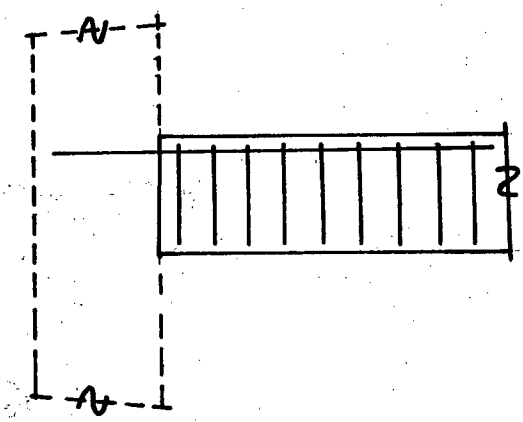

Fig. 1.1c Top Dowel

The experimental investigation consisted of two main series of tests. The first one involved a column specimen and bottom dowel to determine its shear capacity (Fig. 1.1b). The second one involved a beam specimen and a top dowel (Fig. 1.1c). In each series of tests the variable was dowel diameter with sizes ranging from 3/8" to 1-3/8". Once the shear-deflection history of each component part was obtained, the shear capacity of the joint was predicted.

A mode of behaviour (physical model) is presented for each test series and this model is used to predict the behaviour of the steel dowels in shear. The bottom dowel has been modelled as a beam-on-elastic foundation. The top dowel model uses a

transformed section for the steel-concrete interactive behaviour. The details of the experimental program and theoretical analysis will be discussed in the following chapters.

The model for the bottom dowel behaviour required the value for the foundation modulus of concrete K as a function of dowel size. An auxiliary laboratory test program was carried out to establish the K value as a function of dowel diameter. This program is described in detail in Chapter 3.

This investigation on beam-column joints is a continuation of previous work that has been done by Kratz[11] and Peter[1]. Peter's experimental work covered only #3, #5 and #6 dowels and the method of theoretical analysis was in certain cases different from that being presented here. Also, the experimental procedure was different in certain respects. Peter concluded that significant shear capacities are obtained from the dowel action of steel bars.

Birkeland and Birkeland[6] introduced the concept that shear between a concrete to concrete interface is developed by friction and not by bond. The reinforcement across the interface is stressed in tension, thereby providing the normal force which is required across the interface to develop the frictional force.

Mast[2] uses the shear-friction theory in predicting shear transfer across shear planes. The method is applicable to many design problems. A brief description of his method is presented here.

Fig. 1.2a shows a concrete specimen with a crack running perpendicular to the reinforcement.

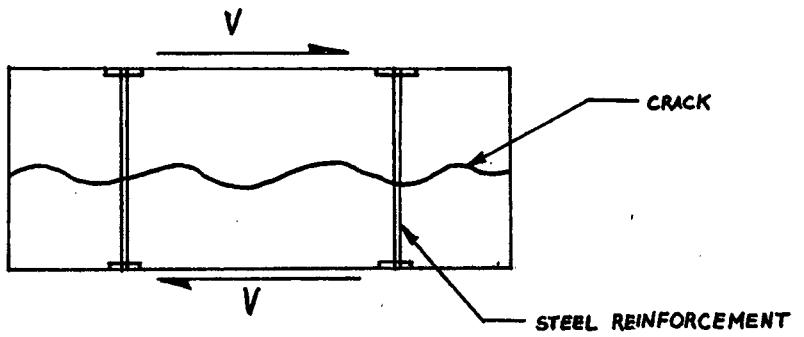

Fig. 1.2a Transverse Crack in Reinforced Concrete Specimen

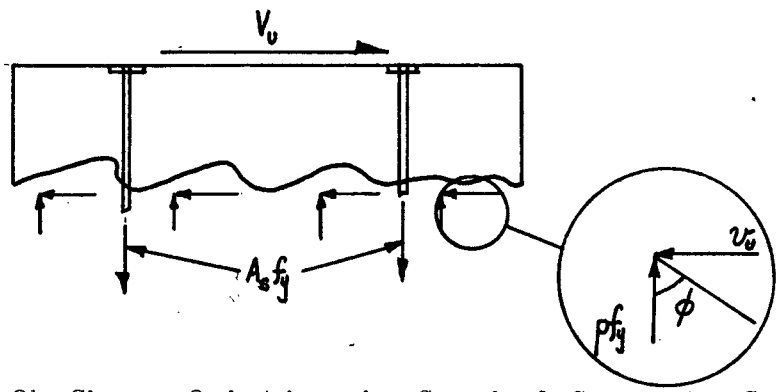

Fig. 1.2b Shear-friction in Cracked Concrete Specimen

Under the action of a shear force V_u, one surface tends to slip relative to the other. As the two surfaces try to separate, the steel is stressed in tension. From the freebody of Fig. 1.2b, the following expression can be formulated:

$$V_u = A_s f_y \tan\phi \qquad (1\text{-}1)$$

$$\text{or} \quad v_u = p f_y \tan\phi \qquad (1\text{-}2)$$

where the steel ratio $p = \frac{As}{bd}$

and ϕ = angle of internal friction for concrete. Mast recommends a range of values for $\tan\phi$ as 0.7 (concrete to concrete and

smooth interface) to 1.4 (concrete to concrete and rough interface).

The equations presented above assume that sufficient separation occurs at the interface to strain the steel to the yield point. As an example, for #5 bars of intermediate grade steel, a separation of 0.01 inches is required to stress the bars to their yield point. Mast also notes some limitations on his theory in order to prevent unsafe extrapolation beyond current knowledge. The value of ϕ has been assumed to be independent of concrete strength and the stress level at the cracked interface. Since this may not actually be so, Mast limits the term pf_y to 15% of the concrete cylinder strength f'_c. He also recommends that #6 bars (intermediate grade steel) be taken as an upper limit in shear friction design.

Hofbeck, Ibrahim and Mattock[3] investigated the shear transfer strength of reinforcing dowels (stirrups) crossing a shear plane. Concrete specimens with and without initial cracks along shear planes were experimentally tested. When the concrete specimens had an initial crack along the shear plane, there was considerable contribution to shear transfer strength by dowel action. For uncracked specimens, the reinforcement is put into tension as a truss-like action develops, i.e., a saw-tooth action as one face tries to slip relative to the other.

The shear-friction design concept, as proposed by Mast, has been successfully applied to several design situations of which the author is familiar. In one instance, a precast load bearing beam-panel was dowelled into a cast-in-place column. Due

to shrinkage, it was feared that the two concrete surfaces may separate and friction would not develop between the two surfaces. In the hope of preventing this, the cast-in-place column was revibrated within 90 minutes of the initial pour in order to "squeeze-out" the excess water and thus minimize shrinkage.

In such cases as described above, it may be useful to consider the dowel action of the steel bars and design the beam-column connection on that basis. The additional work and expense of revibration could be avoided. Also, in order to insure shear-friction action, stringent construction tolerances necessitate that the precast units be positioned snugly against the forms of the cast-in-place units.

In certain situations, shear keys are provided in columns against which a beam is later cast. Some design engineers consider this a very stiff connection and an ideal area for stress concentrations. On the other hand, the design of such beam-column joints on the basis of dowel action provides for a ductile joint as characterized by the shear-deflection behaviour of individual dowels (Appendix 1 and 2).

Many connections are subjected to forces arising from settlement, creep, and shrinkage. These forces are generally unknown and therefore the connection must possess ductility in order to accommodate the additional stresses imposed by these forces.

The following chapters present an experimental and analytical study of dowel action in a beam-column joint and the results of this work are intended to facilitate the design of such connections.

CHAPTER 2. LABORATORY PROGRAM

The laboratory work of forming, casting and curing followed a standard procedure for each test series. This chapter describes the methods involved.

2.1 MATERIAL

All the concrete was delivered by truck from a local ready-mix plant. Type III (High Early) Portland Cement and 3/4" maximum size aggregate was used in the mix. A slump of 3" was specified for each mix.

The deformed bar reinforcing steel was of the type used on construction projects (40 and 60 grade) and was obtained from a local supplier - cut and bent to the required shape. Steel samples were tested in tension to determine yield stress f_y and ultimate stress f_u.

Three concrete cylinders were tested at the beginning of each test series and three at the end. The value of the compressive strength f'_c which was used in the analysis of the test results was an average of the six tests.

The concrete and steel properties for each test series are tabulated in Table 2.1.

2.2 FABRICATION OF TEST SPECIMENS

After the plywood forms were coated with oil, the prefabricated cages of reinforcement were positioned in the forms. During pouring, the concrete was consolidated with a vibrator.

Six companion cylinders (4" x 8") were poured with each test series.

Wet burlap sacks were placed over the poured specimens and everything was covered with a plastic sheet to prevent moisture loss. The burlap sacks were repeatedly moistened everyday. The forms were stripped two days after pouring, but moist curing continued for a total duration of 10 days, after which the plastic and burlap sacks were removed and the specimens left to dry cure on the laboratory floor.

Table 2.1 Concrete and Steel Properties

TEST SERIES		f'_c (Ksi)	f_y (Ksi)	f_u (Ksi)
K TESTS		6.33 for all specimens		
BOTTOM DOWEL TESTS				
Bar Sizes	#3		54	79
	#4		56	80
	#5		66	101
	#6	4.2 for all	71	103
	#7	specimens	73	110
	#8		69	97.5
	#9		69	112
	#10		66.4	102
	#11		66.4	93
TOP DOWEL TESTS				
Bar Sizes	#4	5.675	65	79.5
	#5	3.13	70.5	110
	#6	3.13	66.4	100
	#7	5.675	69.5	110
	#8	3.13	64	104
	#9	5.675	62.7	109
	#10	5.675	62.7	87.5
	#11	6.0	62.7	87.5

CHAPTER 3. FOUNDATION MODULUS OF CONCRETE K

As previously mentioned, the theoretical analysis for the bottom dowels required the value for the foundation modulus of concrete K as a function of dowel size. To determine K for each dowel size, it was decided to test 4 dowel sizes and interpolate for the others. Three specimens were cast for each of dowel sizes #4, #6, #8 and #11. Pouring and curing of concrete followed the standard procedure as described in Chapter 2.

A typical specimen is shown in Fig. 3.1a. Only the bottom-half of the dowel was embedded in concrete. The specimens were tested in a Baldwin loading machine with load and deflection simultaneously recorded on a X-Y plotter. Fig. 3.1b is a schematic representation of the laboratory set-up. Fig. 3.2 shows a specimen in the Baldwin just before the beginning of a test.

The deflection of the steel dowel was measured with linear transformers positioned at each end of the dowel. The x-y plotter recorded the average of the two deflections and also the load which was applied continuously at an average rate of 6 Kips per minute.

There were no visible signs of distress in the concrete specimen until a substantial load was applied. Crushing and spalling of the concrete immediately below the dowel were the first visible signs of progressive failure. For bar sizes #4 and #6, the extent of failure was only crushing of the concrete below the dowel. For the #8 and #11 dowels, the usual crushing and spalling occurred at the initial stages of loading. Also, a

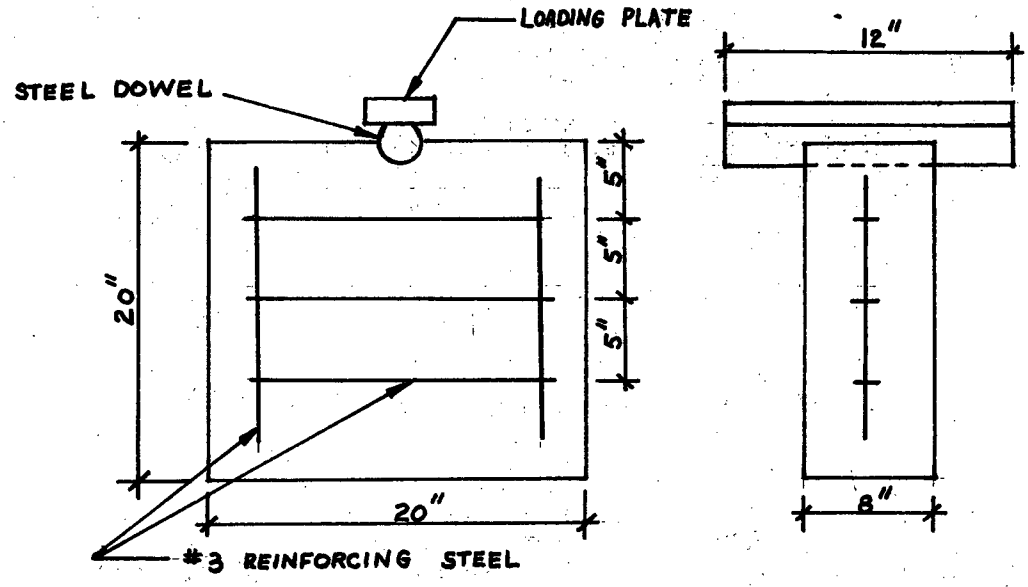

Fig. 3.1a Foundation Modulus Test Specimen

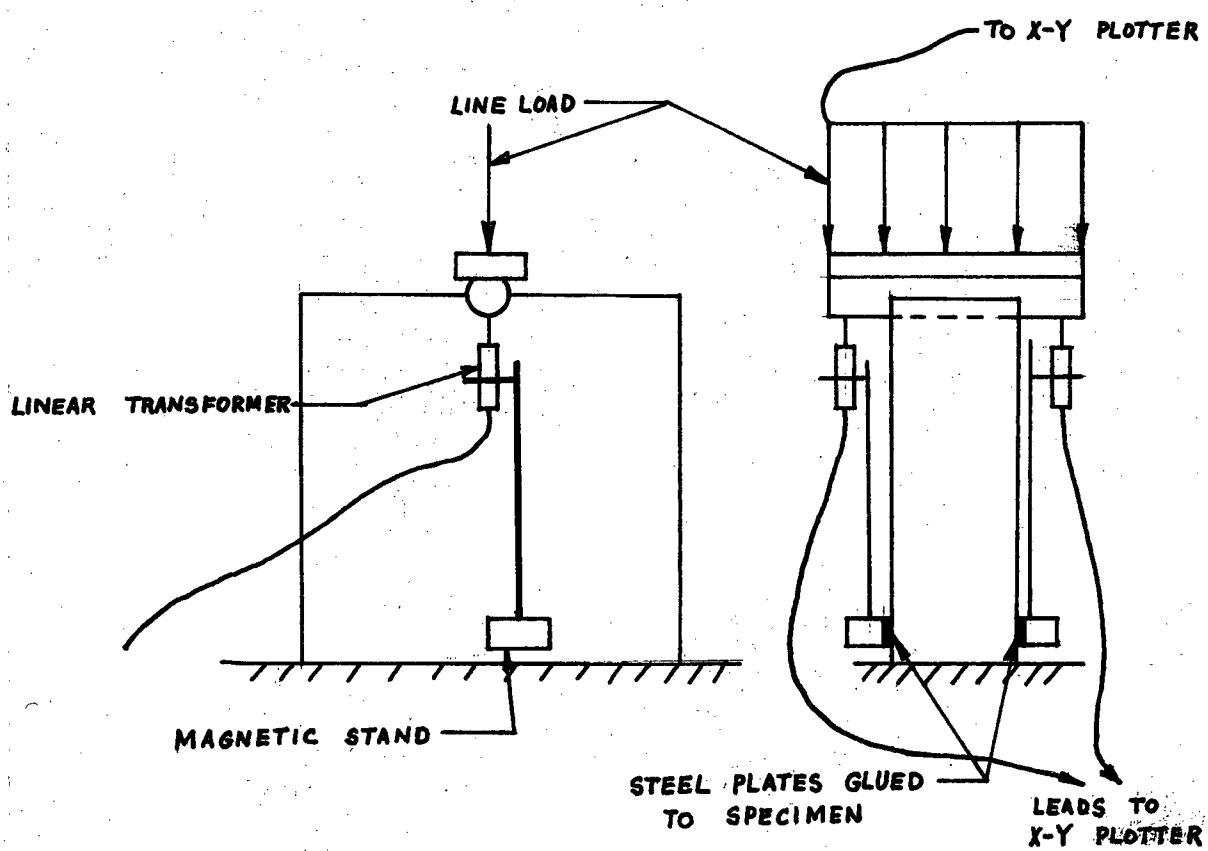

Fig. 3.1b Test Specimen in Baldwin

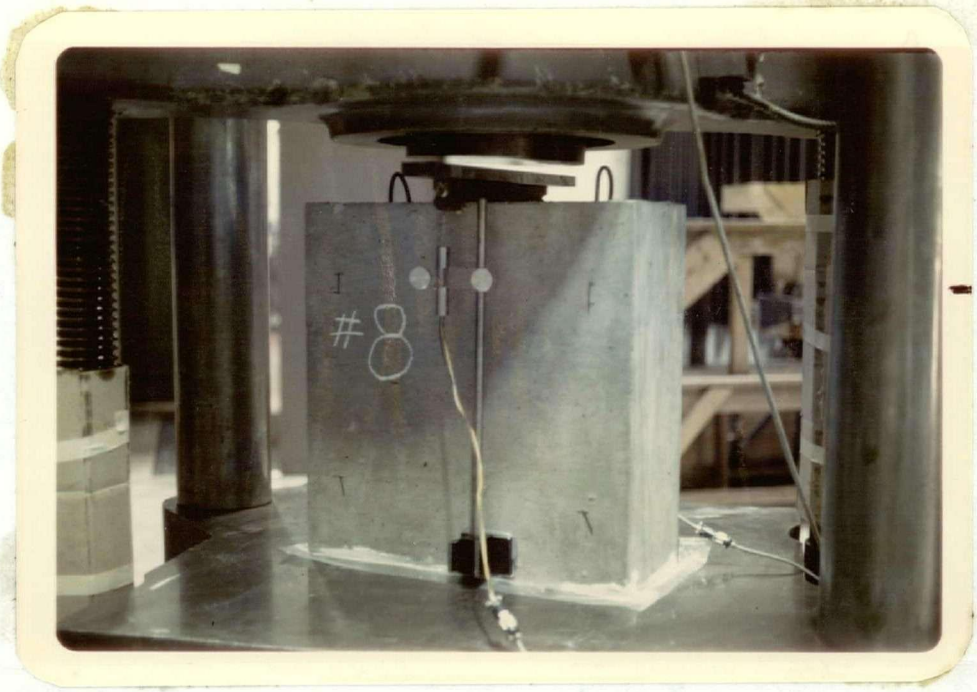

Fig. 3.2 Foundation Modulus Test

Fig. 3.3 Failure of Test Specimen

hairline crack began to propagate vertically downwards and at the completion of the test, the crack had progressed to the base of the specimen.

An "explosive" type of failure was prevented by the horizontal #3 reinforcing bars (Fig. 3.1a). Fig. 3.3 shows the specimen at the end of the test.

The load-deflection graphs for the #8 dowel tests are presented in Fig. 3.4. This set of graphs is typical of the other series. In order to amplify the straight line portion of the graphs, the vertical scale on tests 2 and 3 was doubled. This facilitated in establishing the value for the slope of the graph. The foundation modulus K is calculated by determining the slope of the straight-line portion of the load-deflection graphs and dividing the value by the width of the specimen which was 8 inches.

$$\text{slope} = \frac{\Delta P}{\Delta \delta} \quad \frac{\text{Kip}}{\text{in.}}$$

$$K = \frac{\text{slope}}{8''} \quad \text{Ksi}$$

Therefore the constant K denotes the reaction per unit length of the beam (dowel) where the deflection is equal to unity (Timoshenko[5]).

The results of all the tests are tabulated in Table 3.1. and Fig. 3.5 is a plot of the average K value for each dowel size. The graph was drawn by joining the experimental points.and extrapolating to the #3 dowel size. At each averaged point is a heavy dark line which gives the range in the experimental values.

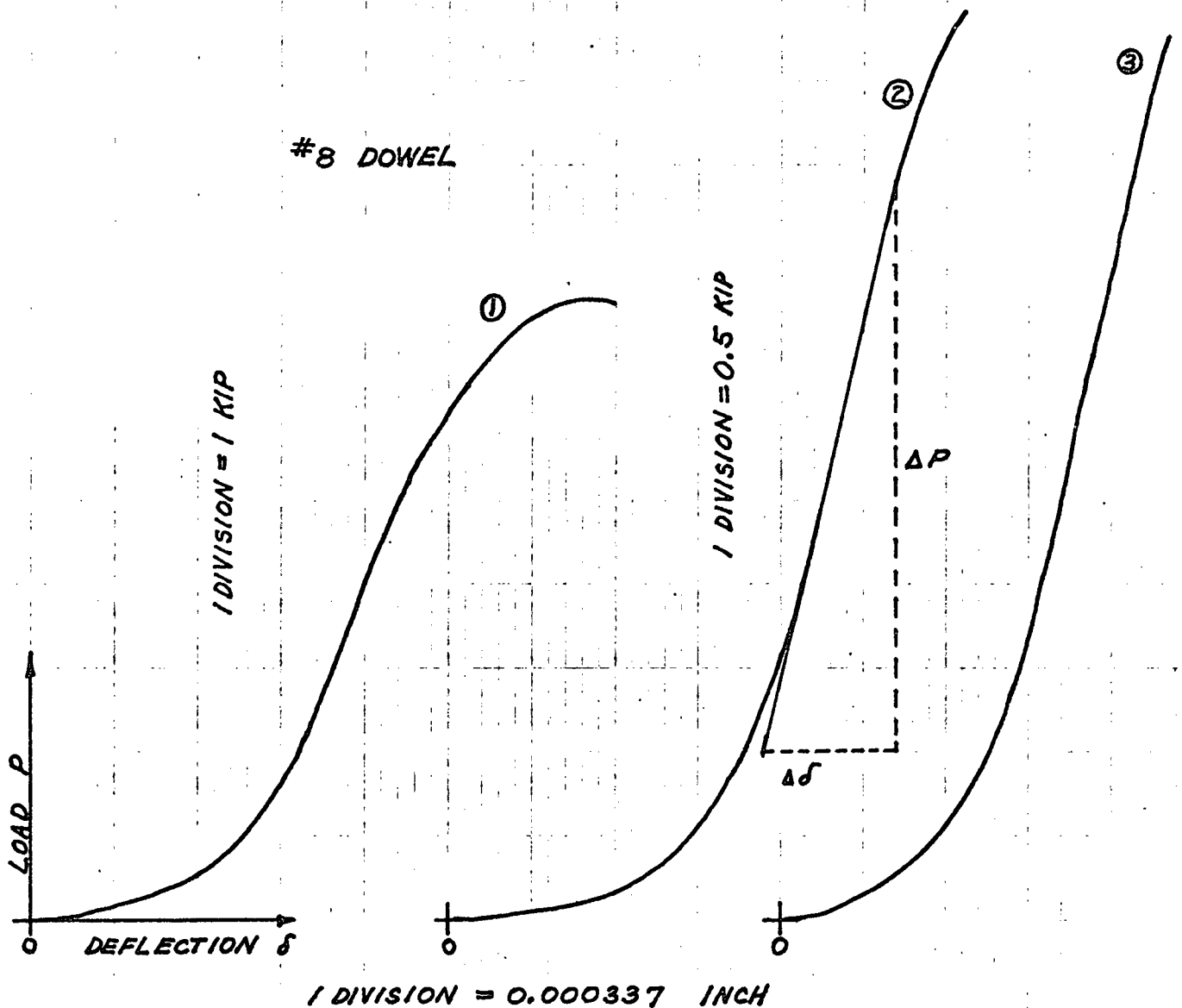

FIG. 3.4 FOUNDATION MODULUS TEST GRAPH

Table 3.1 Foundation Modulus Tests

DOWEL SIZE	TEST NO.	FOUNDATION MODULUS K Ksi	AVERAGE K Ksi
#4	1	512	457
	2	536	
	3	323	
#6	1	820	787
	2	875	
	3	665	
#8	1	925	863
	2	795	
	3	870	
#11	1	1,010	1,005
	2	986	
	3	1,020	

CONCRETE: f_c^1 = 6,330 psi

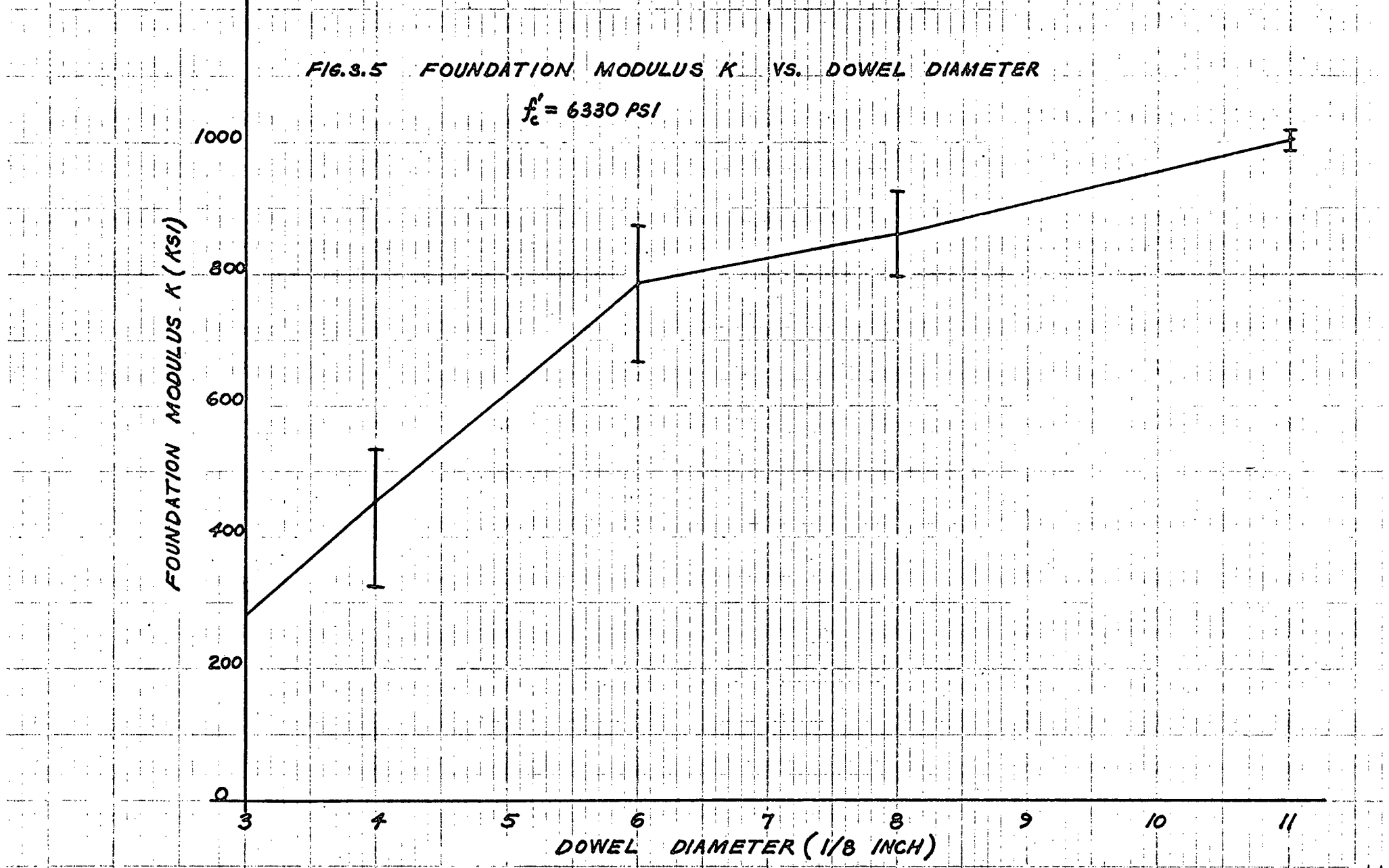
FIG. 3.5 FOUNDATION MODULUS K VS. DOWEL DIAMETER
f'_c = 6330 PSI
FOUNDATION MODULUS K (KSI)
1000
800
600
400
200
0
3
4
5
6
7
8
9
10
11
DOWEL DIAMETER (1/8 INCH)

The graph in Fig. 3.5 is for a concrete strength f'_c of 6,330 psi as determined from the standard cylinder tests. This graph can be scaled for other values of concrete strengths by the following method.

The modulus of elasticity of concrete E_c is a function of $\sqrt{f'_c}$ as given by the empirical equation:

$E_c = 33w^{3/2}\sqrt{f'_c}$ (w = unit weight of hardened concrete in pcf) and the foundation modulus K varies directly with E_c.

Therefore $\frac{K_2}{K_1} = \sqrt{\frac{f'_{c_2}}{f'_{c_1}}}$ or $K_2 = \sqrt{\frac{f'_{c_2}}{f'_{c_1}}}\ K_1$

The factor for scaling the graph of Fig. 3.5 to other concrete strengths is

$$\sqrt{\frac{f'_{c_2}}{f'_{c_1}}} \quad \text{or} \quad \sqrt{\frac{f'_{c_2}}{6330}}.$$

This has been done for several concrete strengths as shown in Fig. 3.6. The foundation modulus K is not too sensitive to varying concrete strengths since the curves of Fig. 3.6 lie in a narrow band.

FIG. 3.6 FOUNDATION MODULUS FOR VARYING CONCRETE STRENGTHS

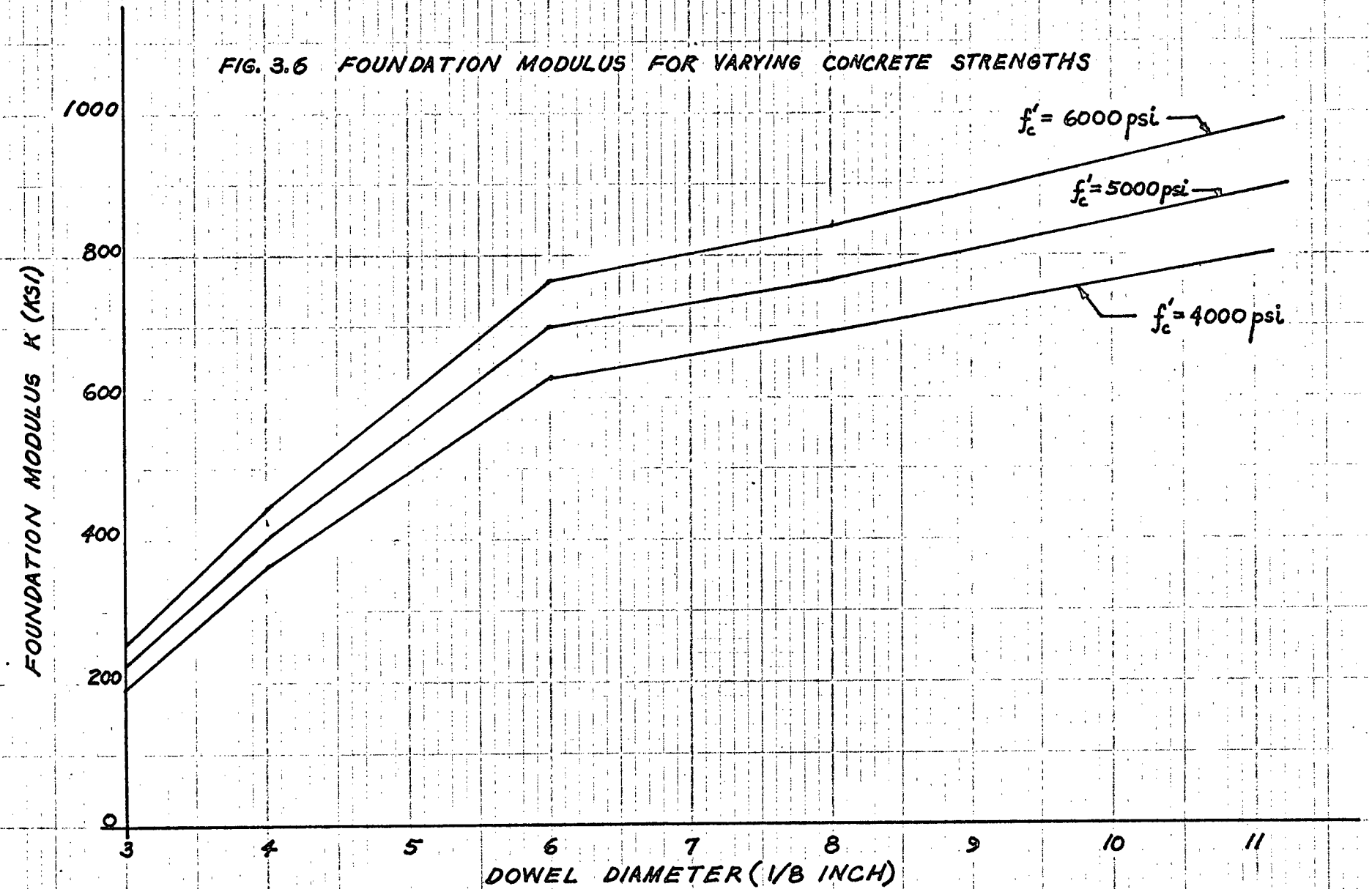

CHAPTER 4. BOTTOM DOWEL TESTS

4.1 EXPERIMENTAL PROCEDURE

In order to determine the shear capacity of the bottom dowels, 36 concrete specimens, as shown in Fig. 4.1, were formed and cast. The variable involved in this study was the dowel size. Four specimens were cast for each dowel size ranging from #3 to #11.

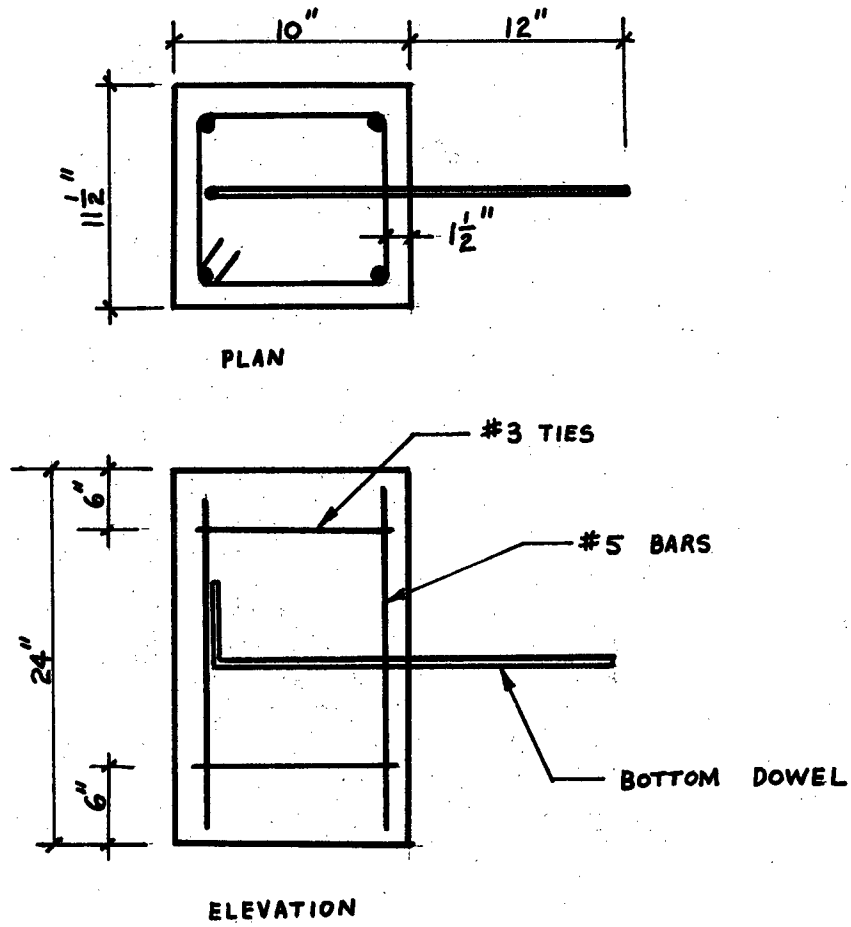

Fig. 4.1 Bottom Dowel Specimen

The method of pouring and curing of concrete was as described in Chapter 2.

It was desired to load the protruding steel dowels in shear only. For this purpose, a wide flange beam was clamped to

the steel dowels and the load applied at the mid-point of the beam. Fig. 4.2 and 4.3 show the positioning of the test specimens (two per test) and the method of load application. The load was applied with an Amsler hydraulic jack. The deflection of the steel dowel was measured at the column face (positions 1 and 2, Fig. 4.2). Since the deflection probes from the transformers were positioned on the dowel itself, the steel clamps were attached 1/4" away from the column face to provide the necessary space for the probes. As a result of this set-up, some bending moment would be developed in the dowel at the column face. This is considered in the theoretical analysis. Linear transformers were again used to measure the deflections and both deflections and load were simultaneously recorded on punched paper tape on a Digital Data Acquisition unit. A computer program converted the paper tape data into the shear-deflection graphs which are presented in Appendix 1. Four curves were obtained for each dowel size.

For simulating the actual column conditions, the concrete column specimens were compressively stressed to 1 Ksi with the tension rods (Fig. 4.2). The force in each tension rod was determined with a strainsert bolt.

4.2 ANALYSIS

The behaviour of the bottom dowel embedded in the concrete column specimen was modelled as a beam-on-elastic foundation. Fig. 4.4b shows a semi-infinite beam on an elastic foundation as discussed in Timoshenko[5]. This model is assumed to represent the section shown in Fig. 4.4a.

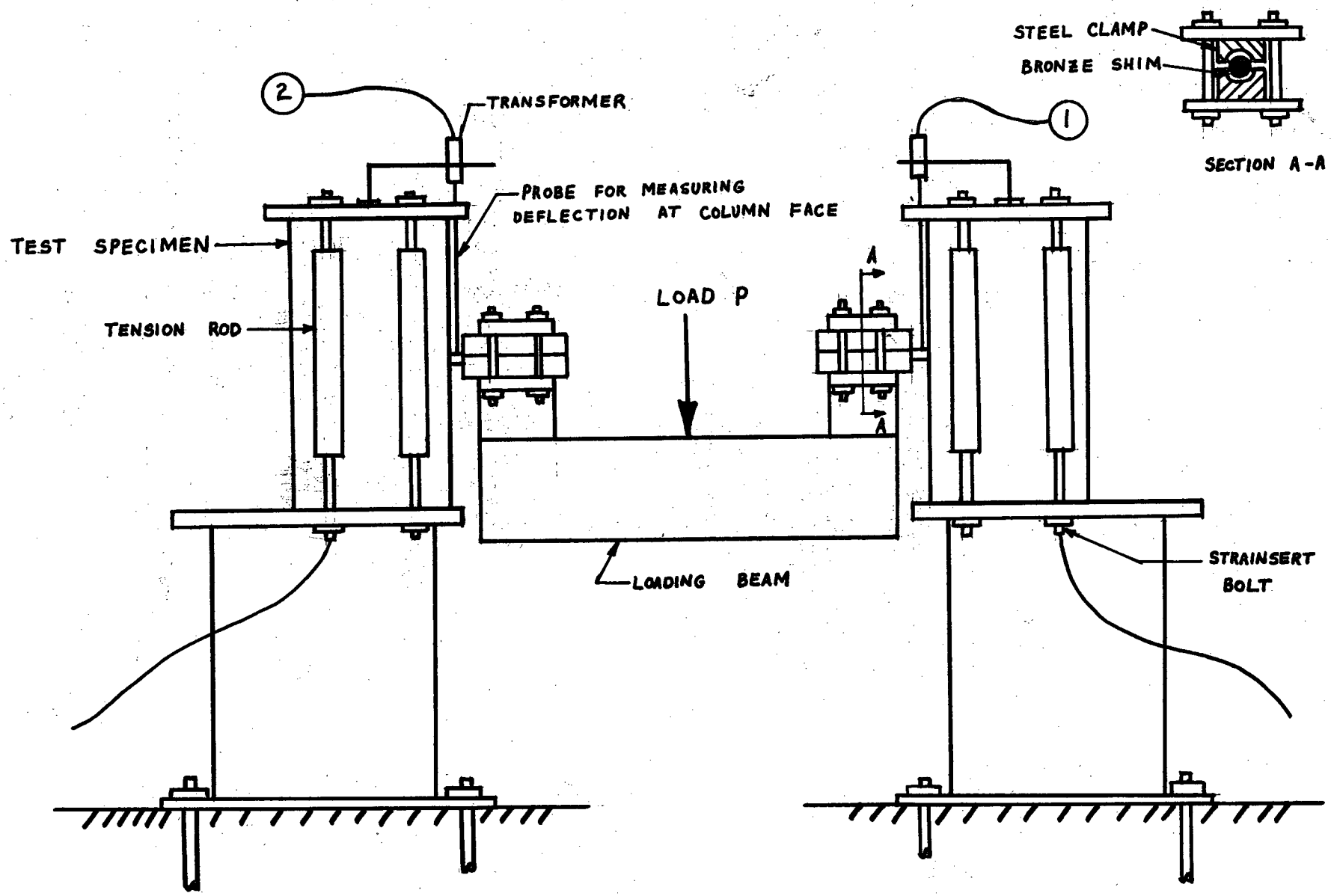

Fig. 4.2 Loading Apparatus For Bottom Dowels

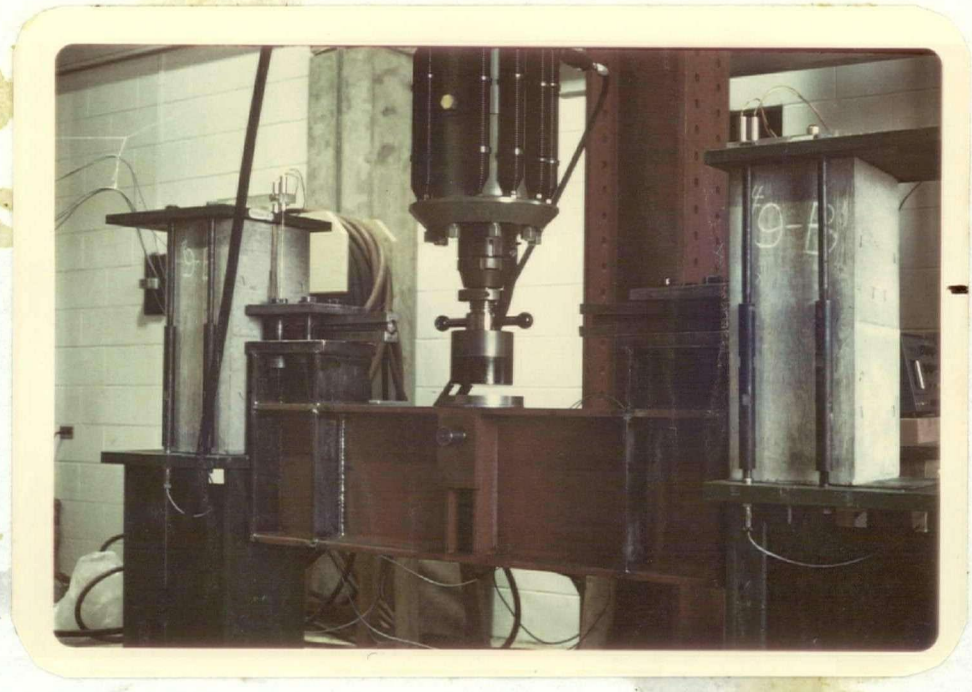

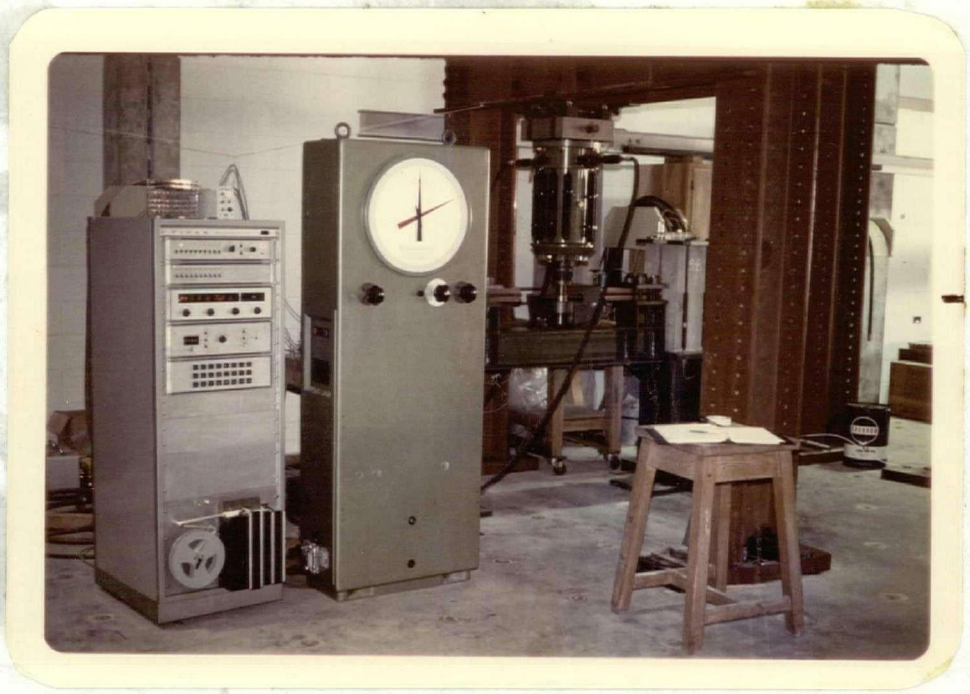

Fig. 4.3 Bottom Dowel Test

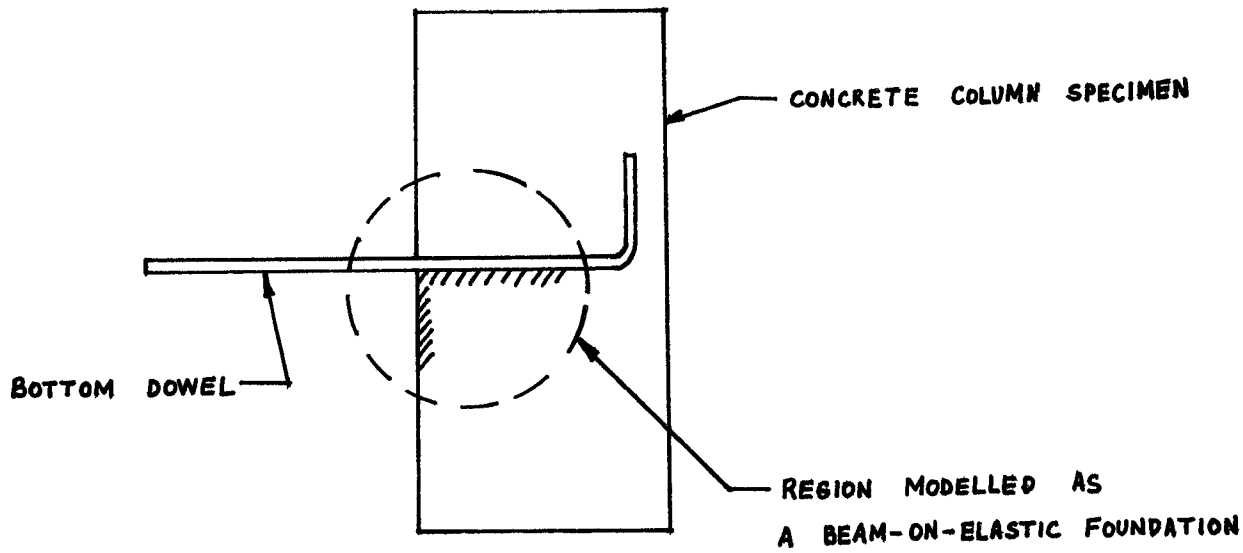

Fig. 4.4a Bottom Dowel Specimen

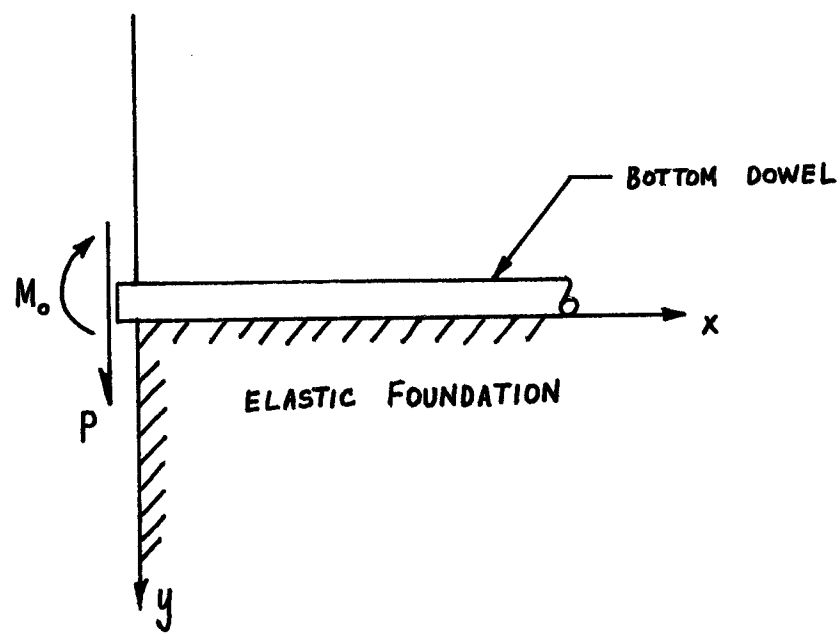

Fig. 4.4b Bottom Dowel Specimen as a Beam-on-elastic Foundation

The solution to the differential equation for a semi-infinite beam on an elastic foundation as shown in Fig. 4.4b is

$$y(x) = \frac{e^{-\beta x}}{2\beta^3 EI}\left(P\cos\beta x - \beta M_o[\cos\beta x - \sin\beta x]\right) \quad (4\text{-}1)$$

where $\beta = \sqrt[4]{\frac{K}{4EI}}$

K = Foundation Modulus

E = modulus of elasticity of the beam

I = moment of inertia of the beam

The values obtained for the foundation modulus in Chapter 3 were used in calculating the β term. Since the bottom dowel specimens had a concrete strength of 4,200 psi, the values for the foundation modulus were scaled by using a factor of

$$\frac{4200}{6330} = 0.815. \quad \text{(Refer to page 17)}$$

The units of K are Ksi and the value for E in all the analysis was 29,000 Ksi (modulus of elasticity of the steel dowels).

To determine the deflection at the column face, the value x = 0 must be substituted into equation 4-1.

$$y(x=0) = \frac{1}{2\beta^3 EI}\left(P - \beta M_o\right) \quad (4\text{-}2)$$

or rearranging

$$P = 2\beta^3 EIy + \beta M_o. \quad (4\text{-}3)$$

As previously mentioned, since some room had to be provided for positioning the deflection probes onto the dowels, the steel clamps were not snug against the column face. Hence, the

bending moment that is developed in the dowel at the column face is opposite in sign to that shown in Fig. 4.4b. With the change in sign, equation 4-3 becomes

$$P = 2\beta^3 EIy - \beta M_o. \qquad (4-4)$$

When M_o is zero, equation 4-4 reduces to

$$P = 2\beta^3 EIy \qquad (4-5)$$

The two extreme values of M_o are zero and M_p - the plastic moment of the steel dowel. Equations 4-4 and 4-5 were superimposed on the shear-deflection curves of dowel sizes #4, #7 and #11, as shown in Fig. 4.5a, 4.5b and 4.5c. The experimental shear-deflection curve is an average of the 4 curves as shown in Appendix 1 for the corresponding dowel size. Table 4.1 lists the variables involved in this analysis.

As can be noted from the graphs, the theoretical curves are below the experimental curve for the #11 dowel up to a deflection of 0.04". As the dowel size is reduced the two theoretical curves shift closer to the experimental curve until the upper line (equation 4-5) begins to exceed the experimental results at a deflection of 0.02" (#4 dowel size).

Fig. 4.6 is a plot of the shear at 0.03" deflection for the range of bar sizes tested. Equations 4-4 and 4-5 are also plotted with the value of "y" equal to 0.03". The majority of the experimental points are bounded.by the two extreme equations. (Heavy dark vertical lines show the range in the experimental results.) Table 4.2 lists the values required in plotting Fig. 4.6. The β term was evaluated for a concrete strength of 4,200 psi.

Table 4.1 Bottom Dowel Variables

Dowel Size	Diameter d (in.)	Moment of Inertia I ($in.^4$)	Foundation Modulus K (Ksi) (for f_c^1 = 4200 psi)	$\beta = \sqrt[4]{\frac{K}{4EI}} \left(\frac{1}{in.}\right)$ (E = 29000 Ksi)	Plastic moment $M_p = 0.167 f_y d^3$ (KIP-IN.)
#3	0.375	0.00097	180	1.13	0.48
#4	0.5	0.00306	372	1.01	1.17
#5	0.625	0.0075	520	0.88	2.7
#6	0.75	0.0155	640	0.77	5.
#7	0.875	0.0286	670	0.67	8.15
#8	1.0	0.049	700	0.59	11.5
#9	1.12	0.0775	730	0.53	16.2
#10	1.25	0.12	770	0.49	21.6
#11	1.38	0.178	815	0.45	29.2

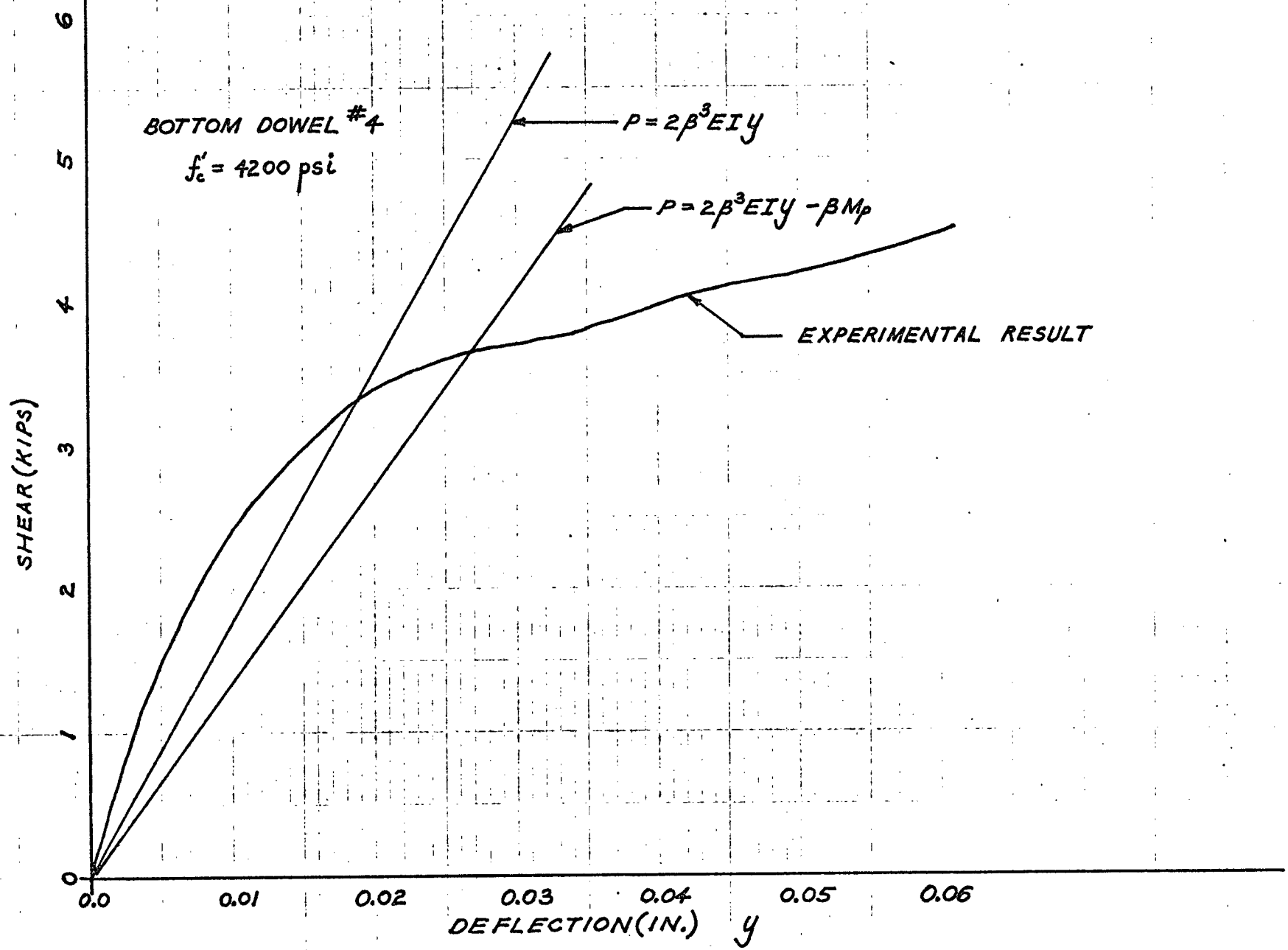
BOTTOM DOWEL #4
f'_c = 4200 psi
$P = 2\beta^3 EIy$
$P = 2\beta^3 EIy - \beta M_p$
EXPERIMENTAL RESULT
SHEAR (KIPS)
0
1
2
3
4
5
6
0.0
0.01
0.02
0.03
0.04
0.05
0.06
DEFLECTION (IN.) y

FIG. 4.5a.

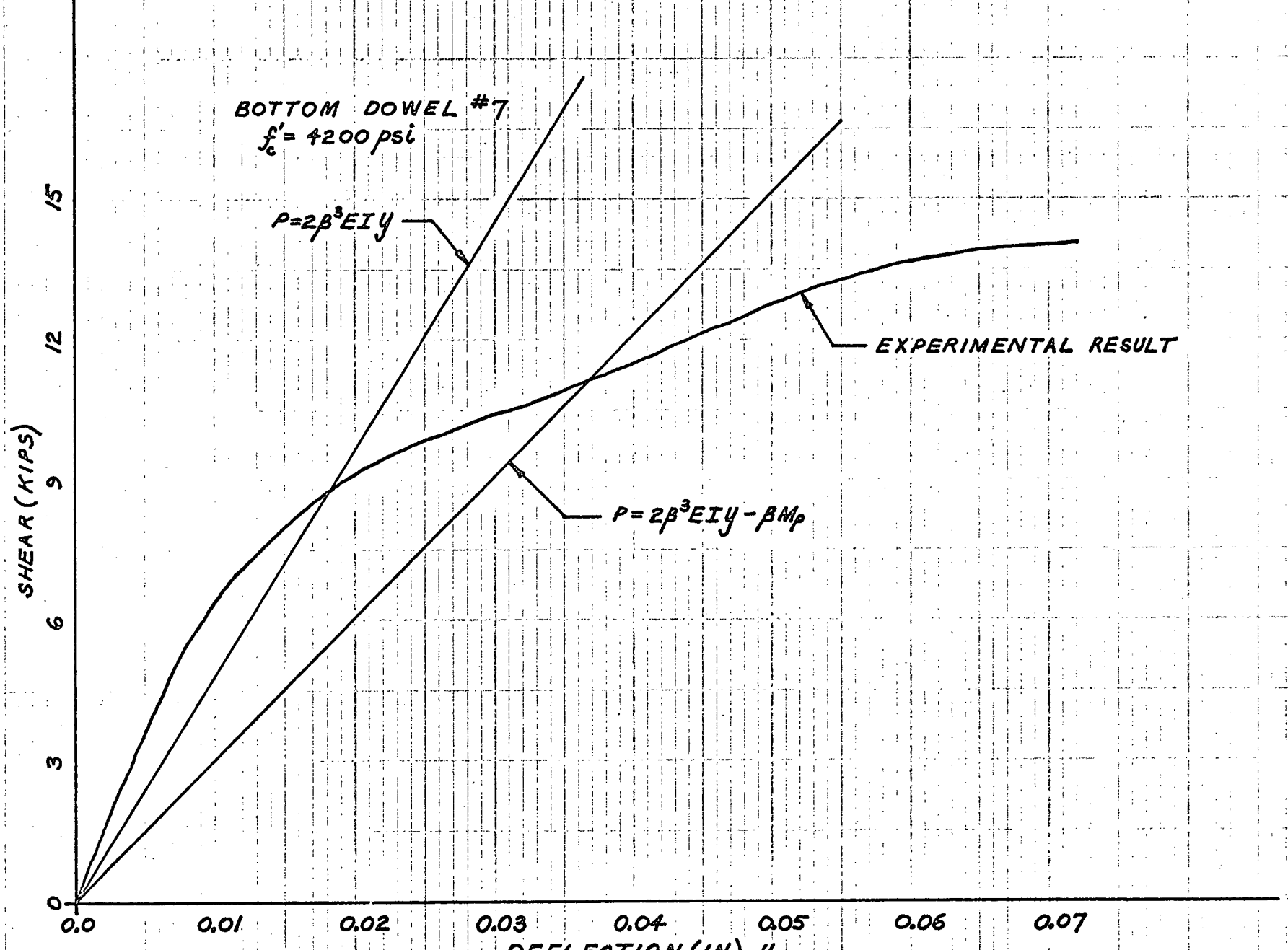
BOTTOM DOWEL #7
f'_c = 4200 psi
$P=2\beta^3EIy$
EXPERIMENTAL RESULT
$P=2\beta^3EIy-\beta M_p$
SHEAR (KIPS)
0
3
6
9
12
15
0.0
0.01
0.02
0.03
0.04
0.05
0.06
0.07
DEFLECTION (IN.) y

FIG. 4.5b.

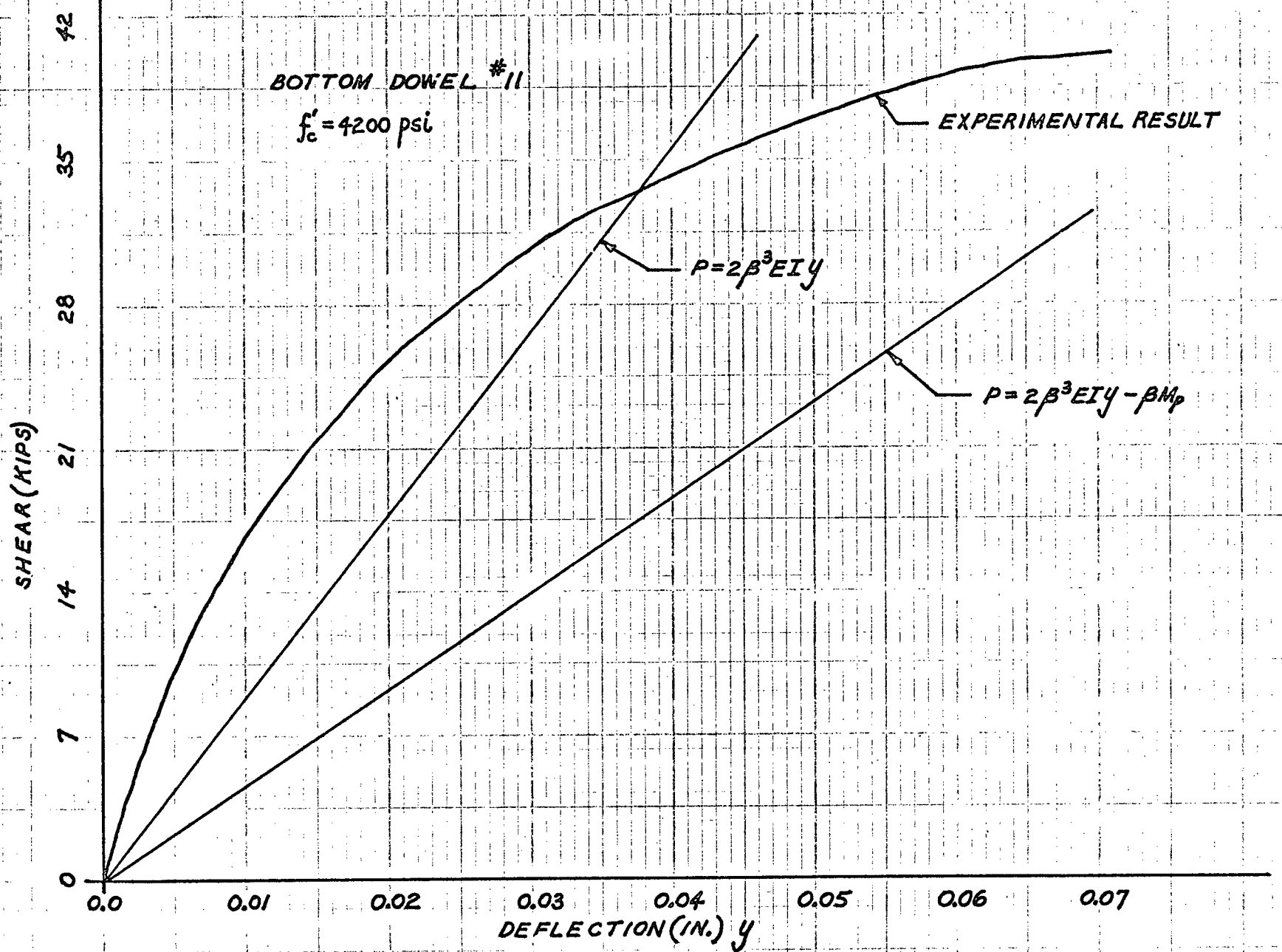
BOTTOM DOWEL #11
$f'_c = 4200$ psi
EXPERIMENTAL RESULT
$P = 2\beta^3 EIy$
$P = 2\beta^3 EIy - \beta M_p$
SHEAR (KIPS)
0
7
14
21
28
35
42
0.0
0.01
0.02
0.03
0.04
0.05
0.06
0.07
DEFLECTION (IN.) y

FIG. 4.5c.

Table 4.2 Shear at 0.03 Deflection

f_c^1 = 4200 psi E = 29000 Ksi y = 0.03"

Dowel Size	Average Shear at 0.03" Deflection (Experiment) (KIPS)	$P = 2\beta^3 EIy - \beta M_p$ (Kips)	$P = 2\beta^3 EIy$ (Kips)
#3	2.5	1.9	2.4
#4	3.6	4.3	5.5
#5	4.9	6.5	8.9
#6	10.4	8.6	12.4
#7	10.4	9.5	15.
#8	13.6	10.9	17.7
#9	18.4	11.9	20.5
#10	27.4	13.3	23.8
#11	30.	14.4	27.4

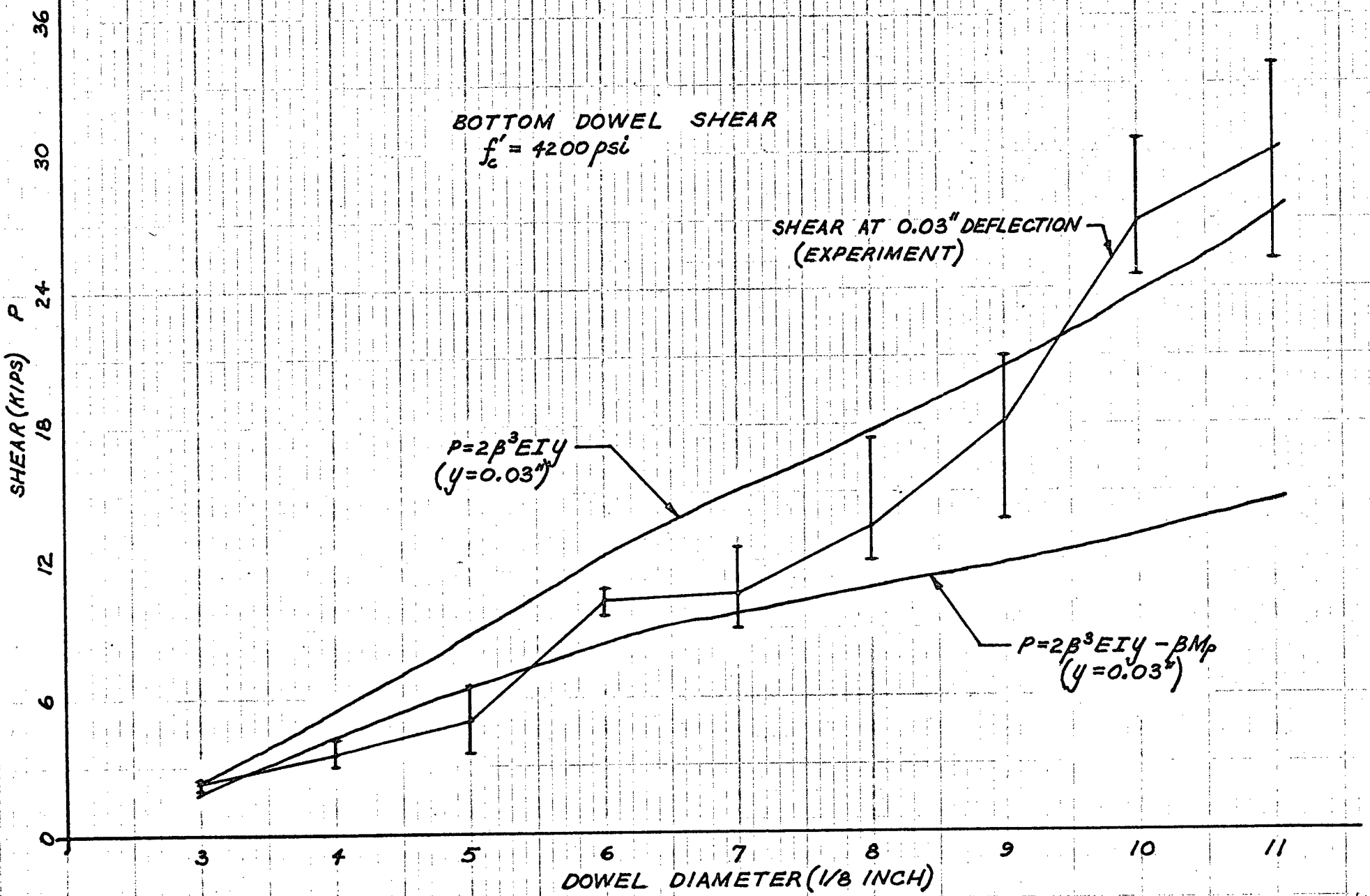
BOTTOM DOWEL SHEAR
$f_c' = 4200$ psi
SHEAR AT 0.03" DEFLECTION
(EXPERIMENT)
$P = 2\beta^3 EIy$
$(y = 0.03")$
$P = 2\beta^3 EIy - \beta M_p$
$(y = 0.03")$
SHEAR (KIPS) P
0
6
12
18
24
30
36
3
4
5
6
7
8
9
10
11
DOWEL DIAMETER (1/8 INCH)

FIG. 4.6

The "knee" of the shear-deflection curves occurs (in most cases) at around the 0.03" value of deflection with the concrete still in the elastic range. At this deflection there were no visible signs of crushing or spalling of the concrete around the dowel. Thus, for this reason the theoretical beam-on-elastic foundation equation was compared to the 0.03" value. Extrapolating the equation to higher values of deflection would result in overestimating the shear capacity, since the concrete under the dowel begins to crush and crack and the shear-deflection curves assume a shallower slope.

Nevertheless, the experimental and theoretical values are in close agreement at the 0.03" value for the entire range of dowel sizes, with some sizes experiencing more deviation than others.

Fig. 4.7 is a plot of equation 4-5 for varying values of concrete strengths. As was shown in Fig. 3.6, the foundation modulus K is not very sensitive to differences in concrete strength. Hence the β term is also rather insensitive to concrete strength, with the result that the two graphs (Fig. 4.7) do not have much variation. For a 50% increase in concrete strength the maximum increase in shear capacity (for a #8 bar) is about 17%.

The ultimate shear for each dowel was taken to be the stage at which the concrete was crushing under the dowel and no increase in load was possible. The ultimate shear and the shear at 0.03" deflection is plotted in Fig. 4.8. In most cases the ultimate shear is double that at 0.03" deflection. A design based on the 0.03" deflection curve would provide a safety factor of 2 in most cases.

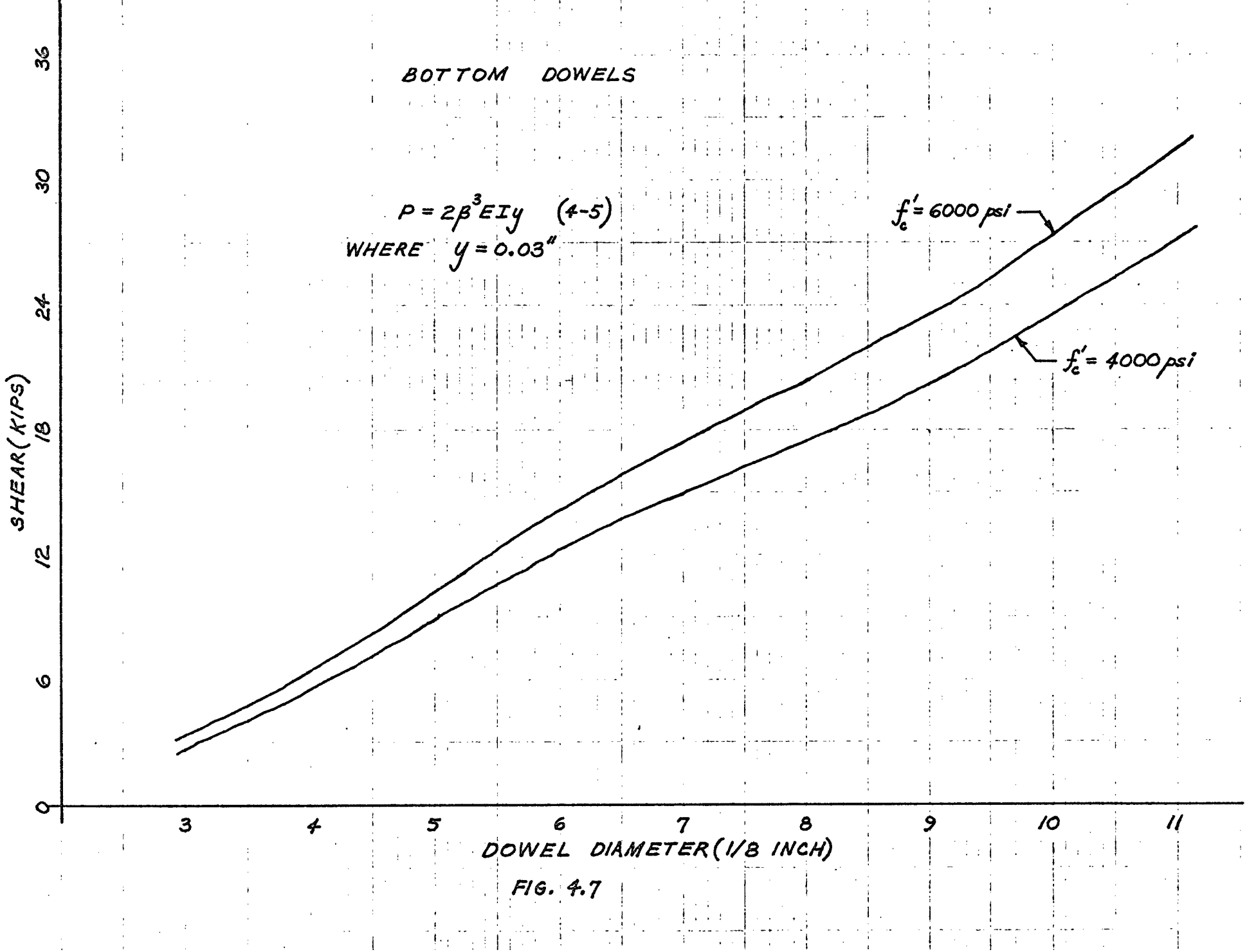
BOTTOM DOWELS
$P = 2\beta^3 EIy$ (4-5)
WHERE $y = 0.03''$
$f_c' = 6000$ psi
$f_c' = 4000$ psi
SHEAR (KIPS)
0
6
12
18
24
30
36
3
4
5
6
7
8
9
10
11
DOWEL DIAMETER (1/8 INCH)

FIG. 4.7

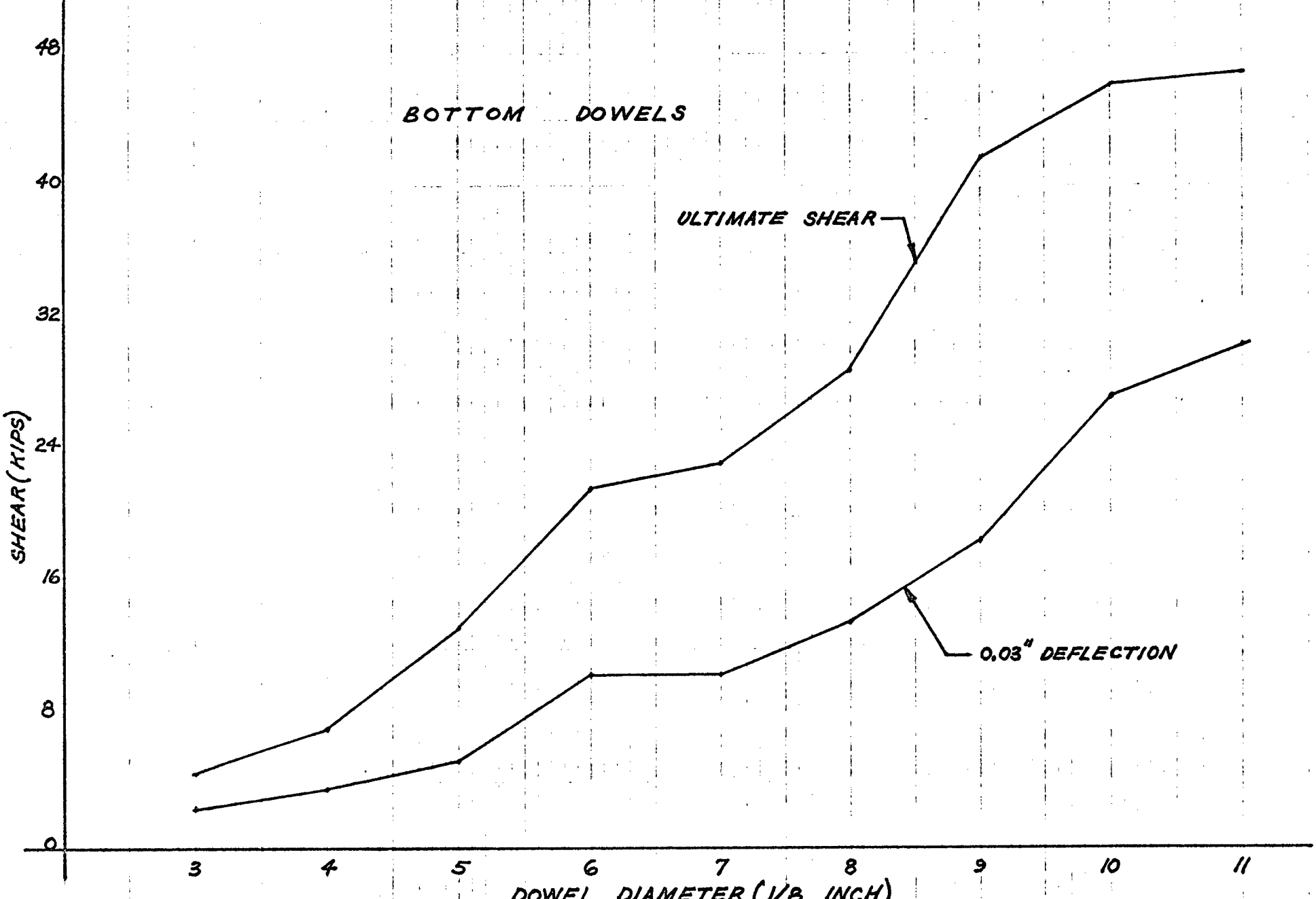
BOTTOM DOWELS
ULTIMATE SHEAR
0.03" DEFLECTION
SHEAR (KIPS)
0
8
16
24
32
40
48
3
4
5
6
7
8
9
10
11
DOWEL DIAMETER (1/8 INCH)

FIG. 4.8

4.3. COMPARISON OF RESULTS WITH PREVIOUS WORK

The results of these tests were compared to previous work which has been done with reinforcing steel dowels and metal studs. Fig. 4.9 presents the experimental results and two expressions from the ACI-ASCE Committee.[9] There the allowable shear for reinforcing steel dowels is given by the expression

$$V = \sqrt{(A_s f_s \cos\theta)^2 + (1.5 d^2 f_c^1 \sin\theta)^2} \qquad (4\text{-}6)$$

where d = sum of the diameter of bars or dowels

θ = angle between beam-column interface and the dowel.

For $\theta = 90°$ (as is the case in this study), the expression reduces to

$$V = 1.5 d^2 f_c^1. \qquad (4\text{-}7)$$

For a metal stud embedded in concrete, the allowable shear is given by

$$V = 110 d^2 \sqrt{f_c^1} \qquad (4\text{-}8)$$

where d = diameter of stud.

Equations 4-7 and 4-8 are plotted and the relative positions of the graphs show that there is a considerable safety factor inherent in these expressions.

Also plotted is Mast's[2] expression

$$V_u = A_s f_y \tan\phi. \qquad (4\text{-}9)$$

Although the method of testing the specimens did not have any shear-friction action, the expression was nevertheless compared to the experimental results by using the lowest value of

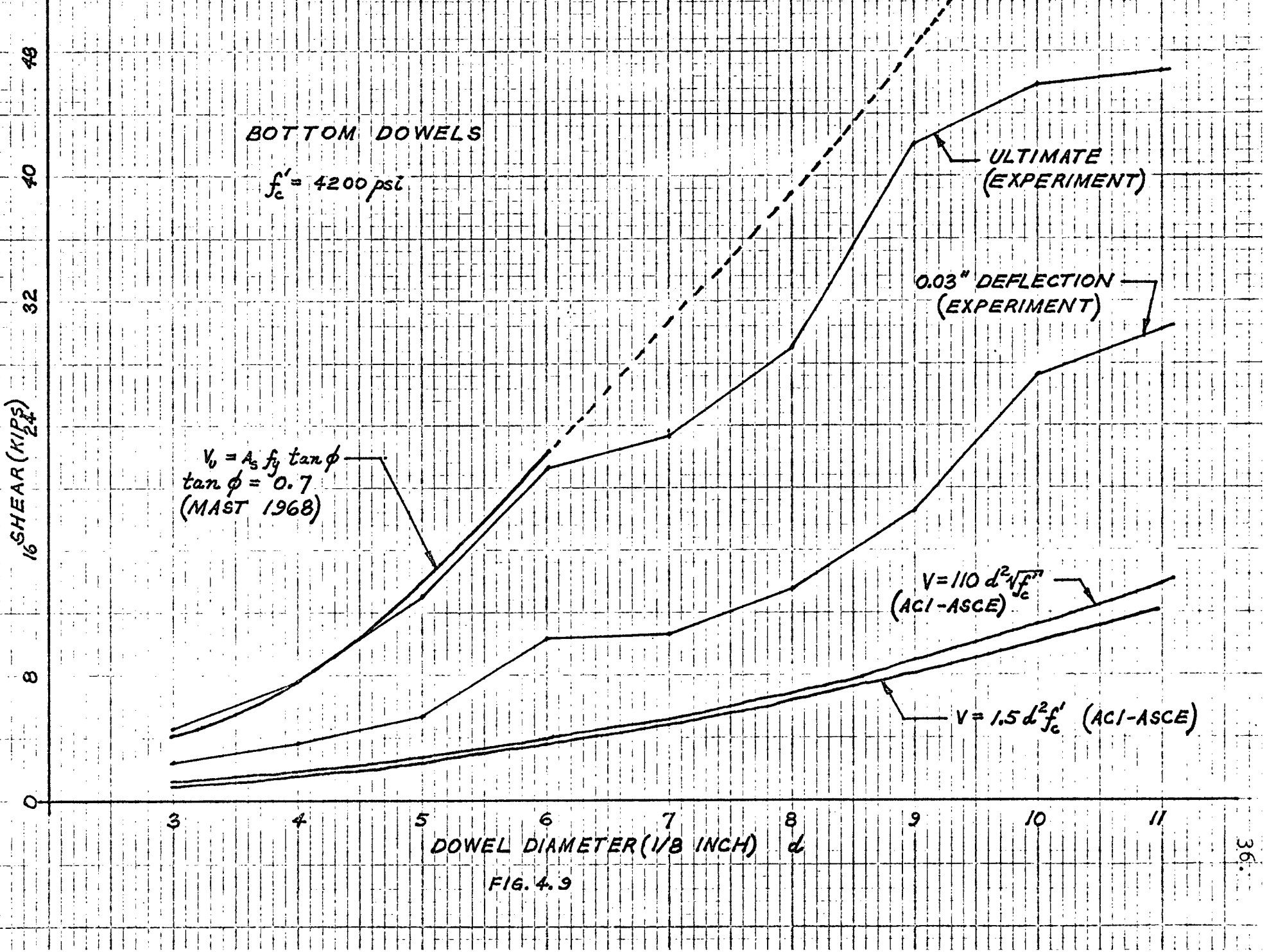
BOTTOM DOWELS
$f_c' = 4200$ psi
ULTIMATE (EXPERIMENT)
0.03" DEFLECTION (EXPERIMENT)
$V_v = A_s f_y \tan\phi$
$\tan\phi = 0.7$
(MAST 1968)
$V = 110\, d^2\sqrt{f_c'}$ (ACI-ASCE)
$V = 1.5\, d^2 f_c'$ (ACI-ASCE)
SHEAR (KIPS)
0
8
16
24
32
40
48
3
4
5
6
7
8
9
10
11
DOWEL DIAMETER (1/8 INCH) d

FIG. 4.9

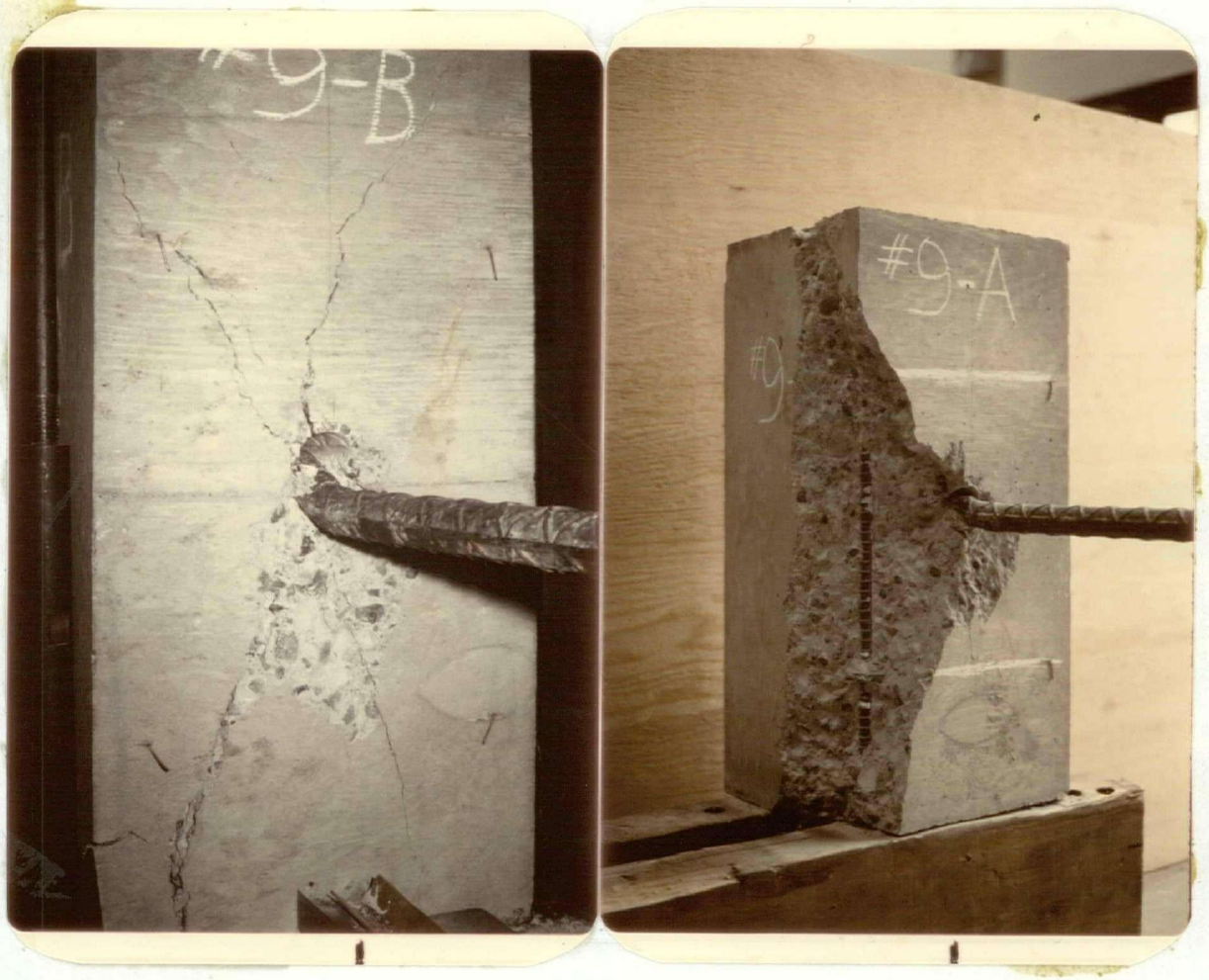

Fig. 4.10 Bottom Dowel Specimens at Ultimate Load

$\tan\phi = 0.7$ as suggested by Mast. There is excellent agreement between Mast's expression and the experimental results up to the #6 dowel. However, extrapolating the equation to the larger dowel sizes results in overestimating the ultimate shear as obtained in this experiment.

Some of the larger dowel sizes reached ultimate deflections of 0.5" to 0.7" (Appendix 1) while the smaller ones ranged between 0.2" to 0.4". An "average" ductility factor μ for an individual dowel (based on the 0.03" deflection value as an elastic or yield limit) would be calculated as

$$\mu = \frac{0.4}{0.03} = 13.$$

Fig. 4.10 shows several specimens at ultimate load and the extent of damage to them. The test specimens had only two column ties (Fig. 4.1) and there was substantial diagonal cracking and spalling of the concrete at ultimate load (Fig. 4.10 and 4.11) for the larger dowel sizes. The smaller sizes experienced only local crushing and spalling under the dowel.

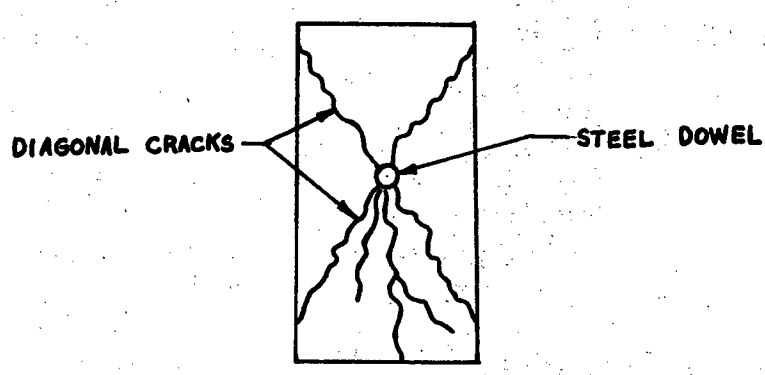

Fig. 4.11 Crack Pattern at Ultimate Load

More column ties should be provided at such beam-column connections to prevent excessive cracking and spalling of the concrete. This hoop reinforcement would provide additional confinement to the concrete and as such increase the ultimate capacity of the dowel.

A study of beam-column connections was conducted by Hanson and Connor[4]. They found that confinement of the concrete at critical sections such as beam-column connections increases the ductility of the joint. The hoop reinforcement resists the tendency of the joint to expand under multiple reversals of beam loading. For joints that are confined on at least three sides by beams or spandrels, hoop reinforcement in the joint region is not required. For unconfined or isolated beam-column joints, hoop reinforcement is most beneficial.

CHAPTER 5. TOP DOWEL TESTS

5.1 LABORATORY TEST PROGRAM

To determine the shear capacity of the top dowels in a beam-column joint, 16 beam specimens were tested. Fig. 5.1 shows a typical beam specimen. Again the variable was dowel diameter. Two such specimens were cast for each bar size - #4 to #11 inclusive. Forming, pouring and curing of the test specimens were done by the standard procedure as outlined in Chapter 2.

The distance from the beam end to the first stirrup was kept constant at 1 inch. A previous study by Peter[1] showed that the shear capacity was significantly influenced by the distance to the first stirrup. He varied the distance from 1 inch to 3 inches and obtained the maximum shear with the 1 inch position. His tests were done for a #5 top dowel only.

To determine if the beam stirrup spacing has any effect on the shear capacity of the top dowel, one-half of the beam had the stirrup spacing as required by the ACI code (318-71) and the other half had double the specified spacing.

The testing apparatus is shown in Fig. 5.2 and Fig. 5.3.

Not shown in Fig. 5.2 are two end roller restraints placed against the sides of the test beam and clamped to the end supports. (These are visible in the photographs, Fig. 5.3.) The rollers prevented the beam from rotating laterally as the load was applied.

Deflections were measured with linear transformers at

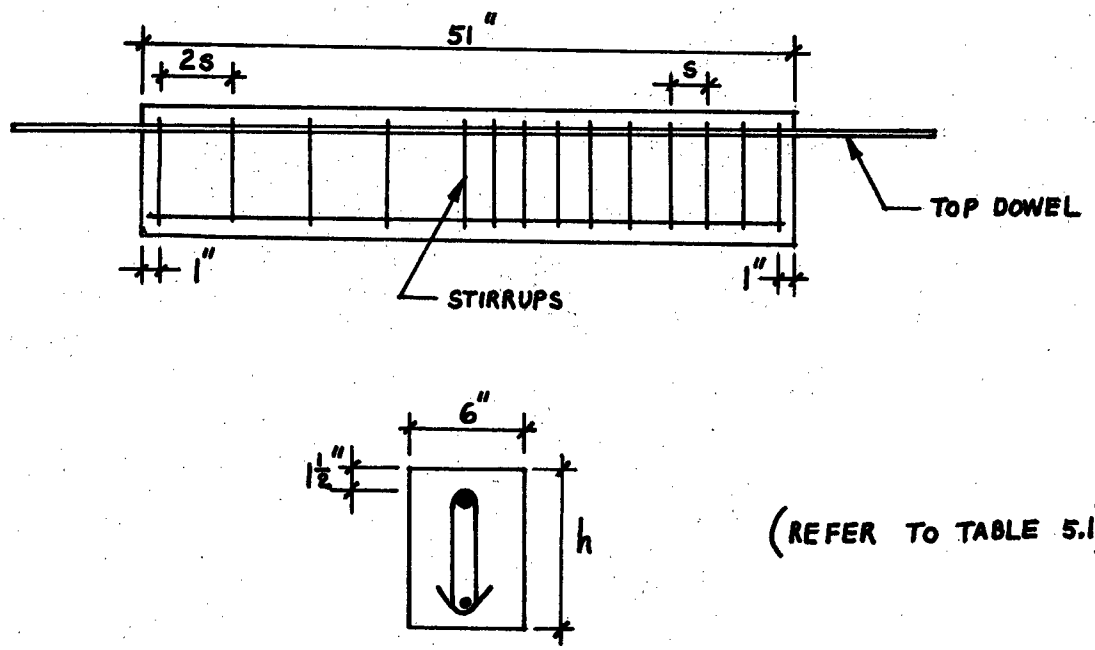

Fig. 5.1 Top Dowel Specimen

Table 5.1 Top Dowel Test Specimens

Top Dowel Size	S (In.)	h (in.)	Stirrup Size
#4	5	12	#3
#5	5	12	#3
#6	5	12	#3
#7	5	12	#3
#8	3½	16	#3
#9	6	16	#4
#10	3½	16	#4
#11	3½	16	#4

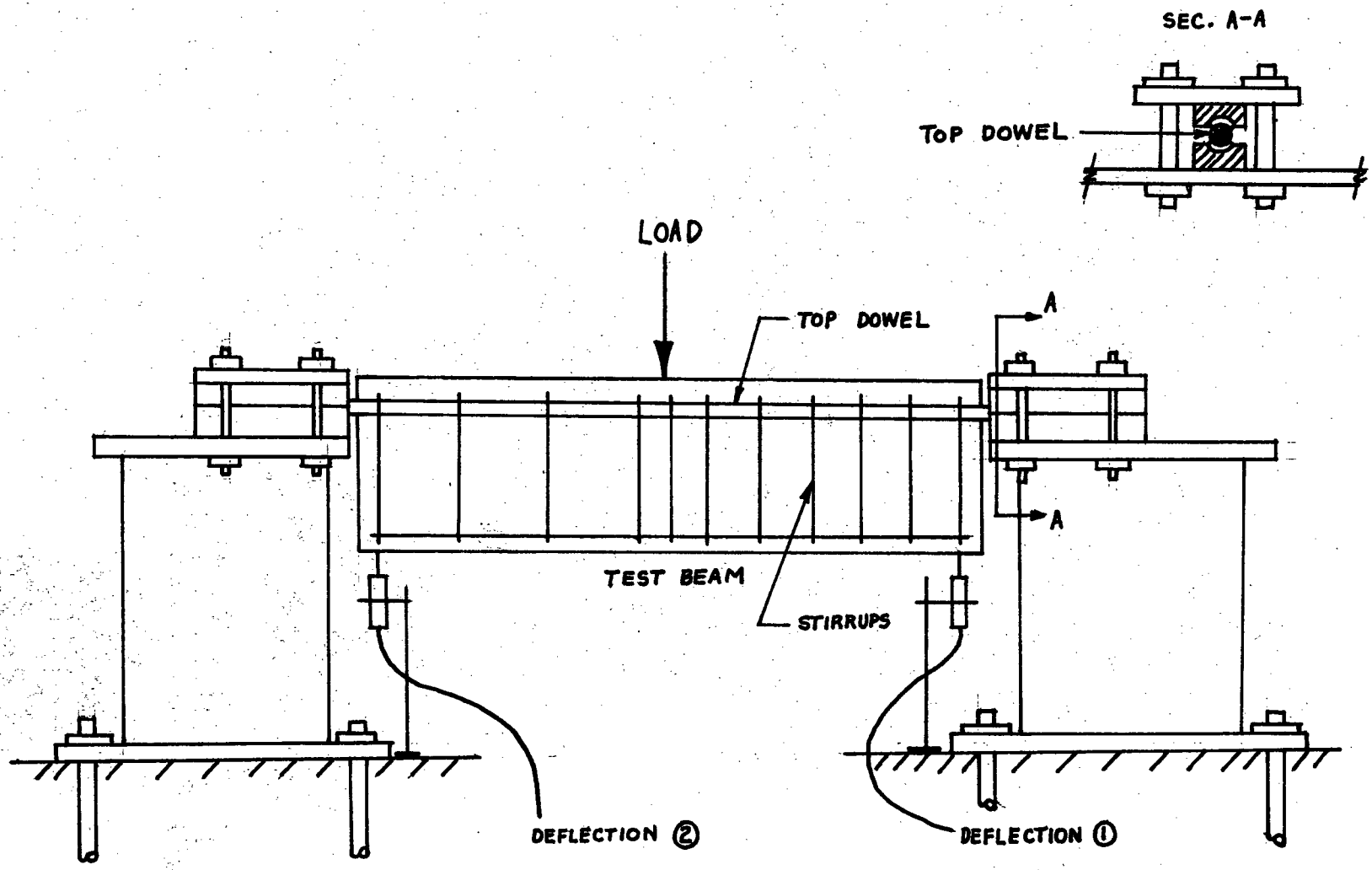

Fig. 5.2 Top Dowel Test Apparatus

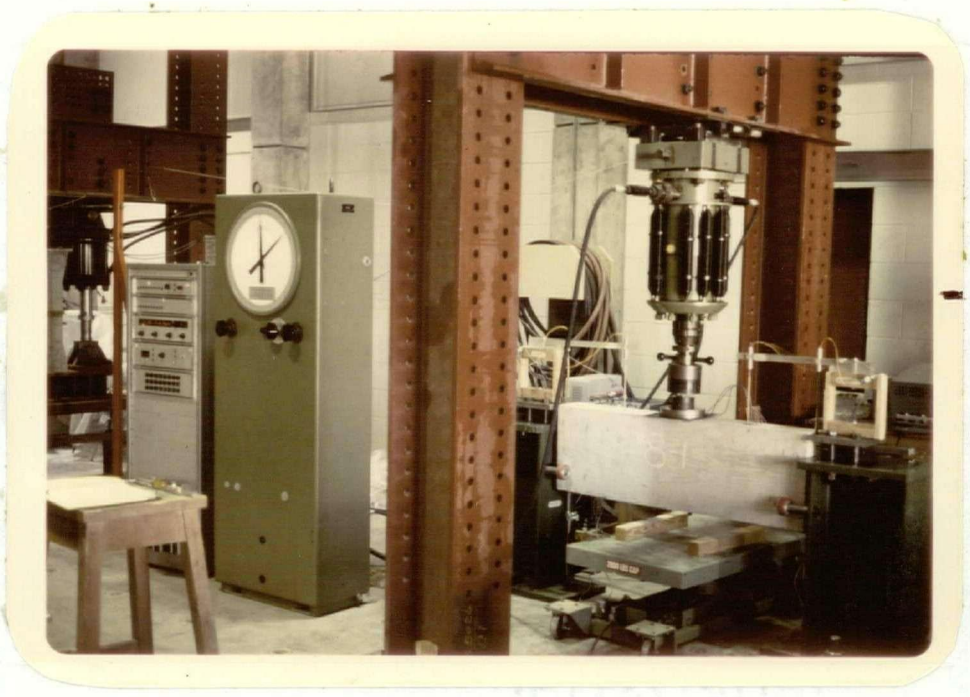

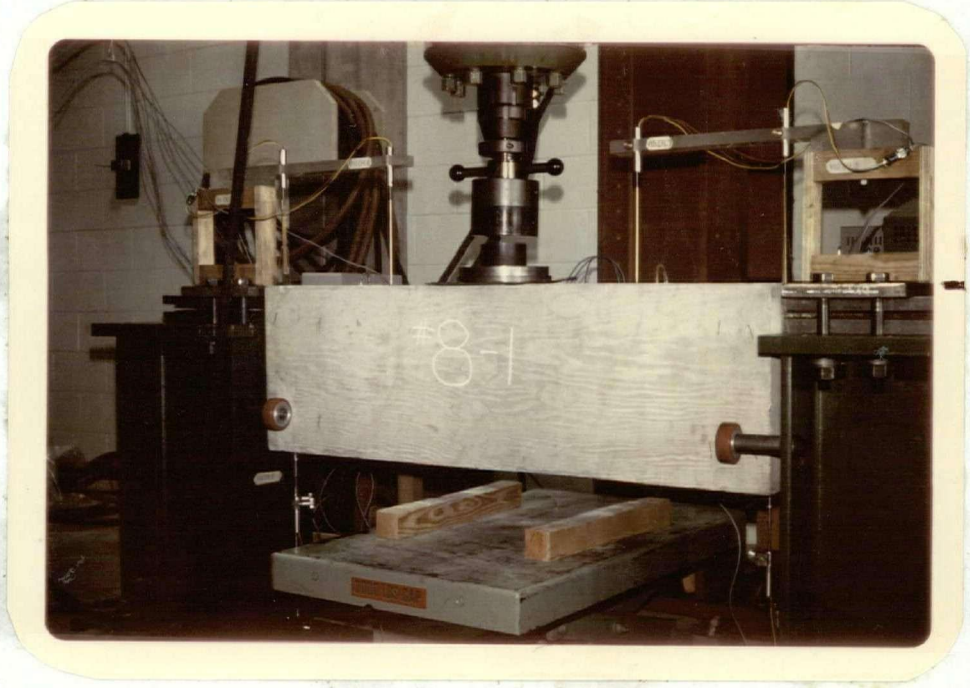

Fig. 5.3 Top Dowel Test

positions 1 and 2 (Fig. 5.2) and both load and deflections were recorded on punched paper tape. As before, a computer program converted the punched paper tape data into the shear-deflection graphs which are presented in Appendix 2.

5.2 ANALYSIS

As in the bottom dowel analysis, a model was chosen for the top dowel behaviour. Fig. 5.4 shows the end region of the test beam with a shear force V applied to the dowel at the beam end. In order to analyze this end region as a unit, the section is transformed as shown in Fig. 5.5.

If the section shown in Fig. 5.5 is assumed to act as a 1" long cantilever beam, the moment that is developed before the section ruptures in tension is

$$M = \frac{f_r I_t}{y_b} \qquad (5\text{-}1)$$

where the modulus of rupture of concrete $f_r = 7.5\sqrt{f'_c}$,

I_t = moment of inertia of transformed section

and y_b = distance from the neutral axis of the transformed section to the extreme fiber in tension.

With the concentrated load V at the end of the cantilever

$$M = V*1"$$

or

$$V*1" = \frac{f_r I_t}{y_b}. \qquad (5\text{-}2)$$

Table 5.2a lists all the variables required to plot equation 5-2. Fig. 5.6a shows the experimental results and a

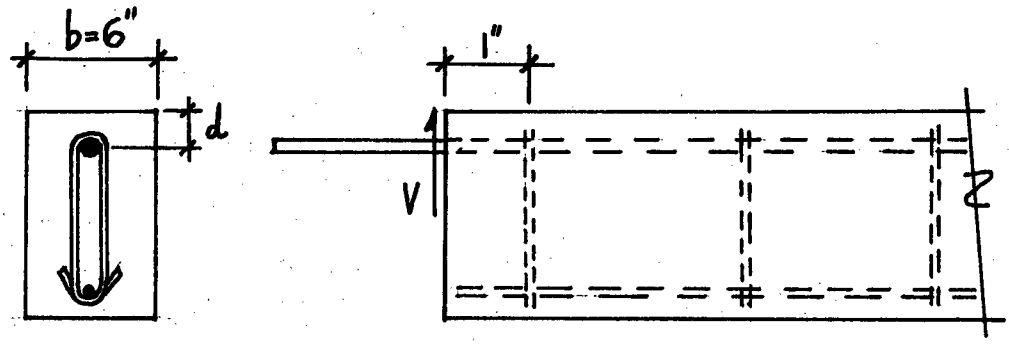

Fig. 5.4 Shear V acting on Top Dowel

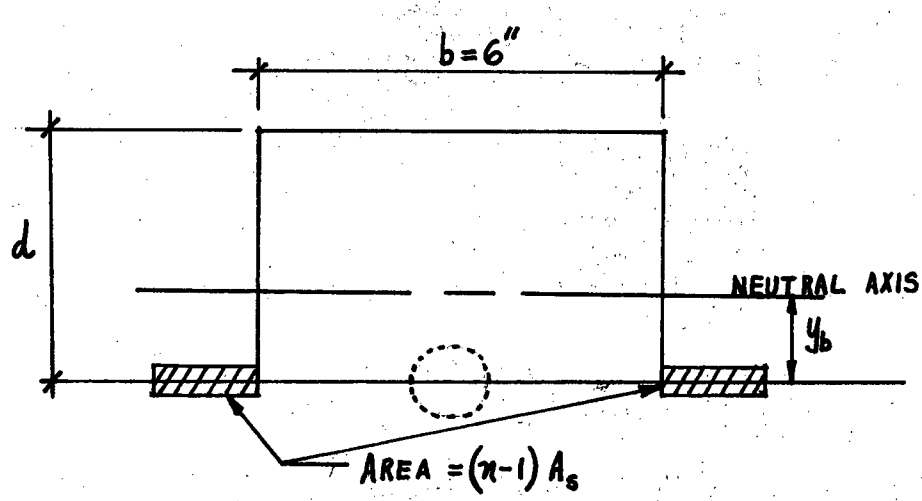

A_s = AREA OF TOP DOWEL

MODULAR RATIO $n = \frac{E_s}{E_c} = 10$

Fig. 5.5 Transformed Section

Table 5.2a Transformed Section Properties

Top Dowel Size	$f_r = 7.5\sqrt{f'_c}$ (Ksi)	I_t ($in.^4$)	Y_b (in.)	$V = \frac{f_r I_t}{Y_b}$ (Kips)
#4	0.565	3.86	0.75	2.9
#5	0.42	4.8	0.72	2.8
#6	0.42	6.08	0.71	3.6
#7	0.565	7.73	0.69	6.3
#8	0.42	8.46	0.63	5.65
#9	0.565	9.14	0.57	9.
#10	0.565	11.9	0.55	12.2
#11	0.580	13.57	0.54	14.6

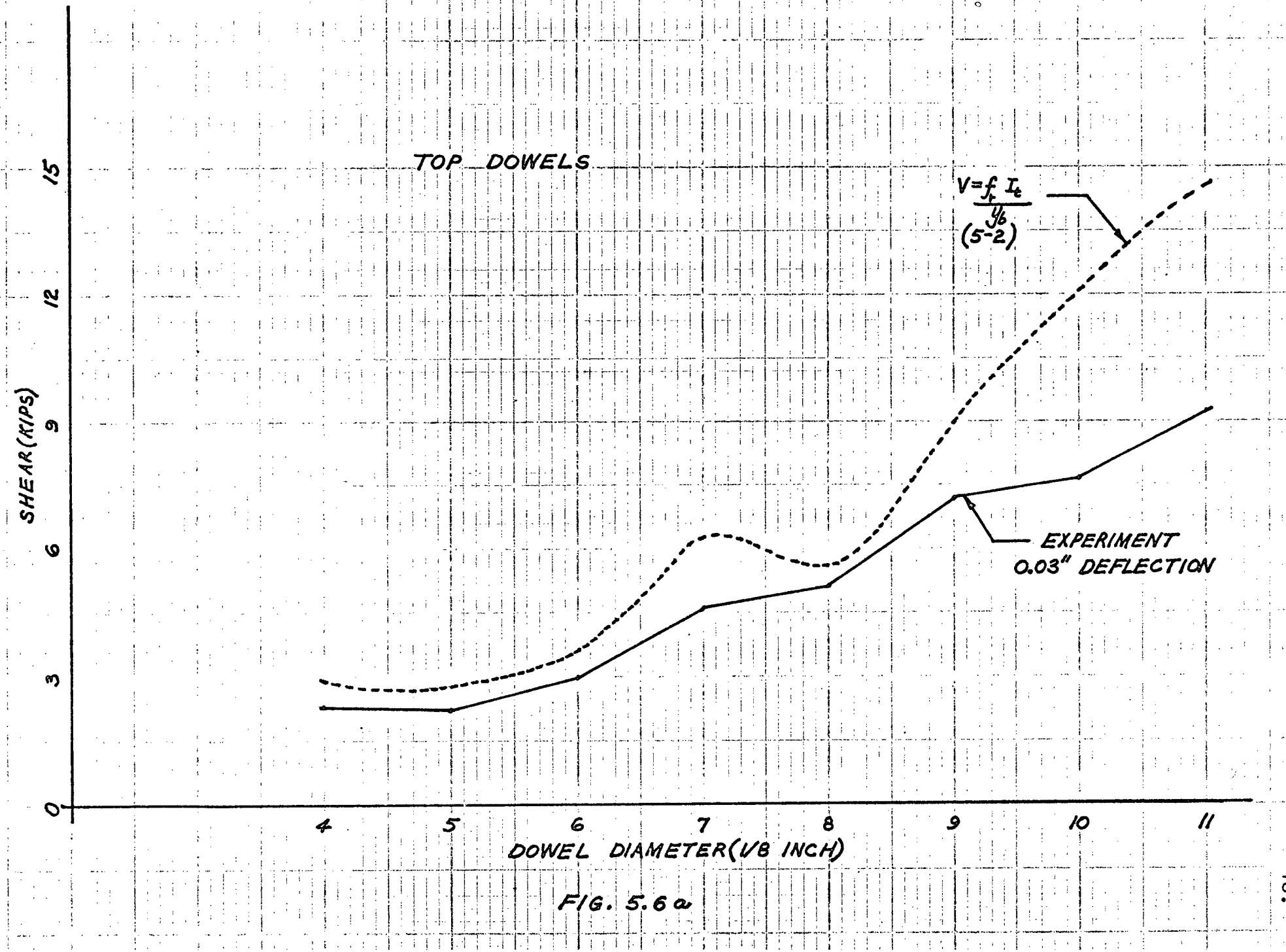
TOP DOWELS
$V=\frac{f_t I_t}{y_b}$
(5-2)
EXPERIMENT
0.03" DEFLECTION
SHEAR (KIPS)
0
3
6
9
12
15
4
5
6
7
8
9
10
11
DOWEL DIAMETER (1/8 INCH)

FIG. 5.6a

Table 5.2b Normalized Experimental Results

Dowel Size	$V = \frac{f_r I_t}{Y_b}$ (KIPS)	f'_c Ksi	$\frac{V}{f'_c}$	Vexp. Shear at 0.03" Defln. (KIPS)	$\frac{Vexp.}{f'_c}$
#4	2.9	5.675	0.511	2.34	0.412
#5	2.8	3.130	0.894	2.34	0.747
#6	3.6	3.130	1.15	3	0.96
#7	6.3	5.675	1.11	4.5	0.79
#8	5.65	3.13	1.81	5.1	1.63
#9	9	5.675	1.58	7.2	1.27
#10	12.2	5.675	2.15	7.5	1.32
#11	14.6	6.0	2.43	9.3	1.55

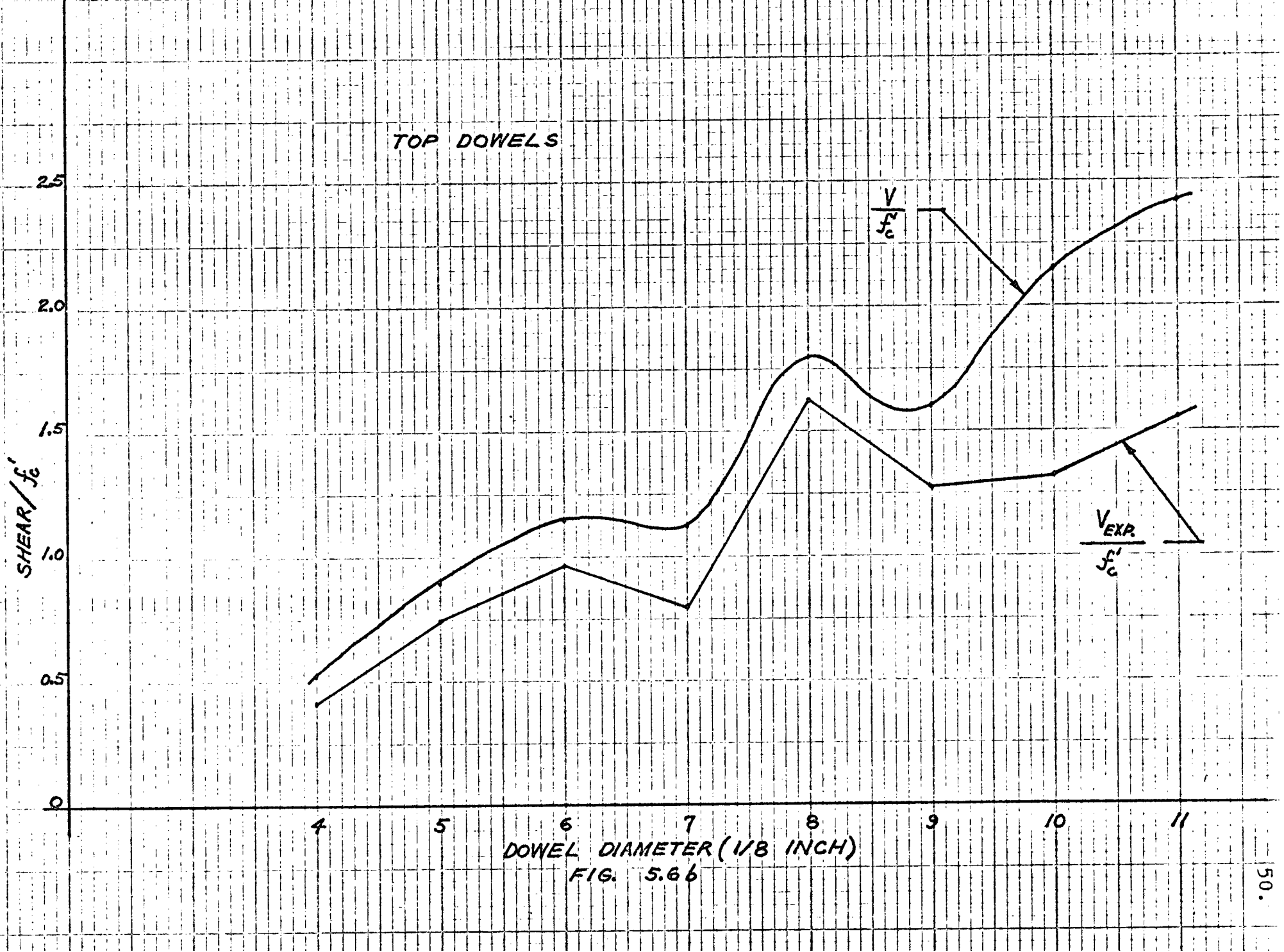
TOP DOWELS
2.5
2.0
1.5
1.0
0.5
0
SHEAR / f_c'
$\frac{V}{f_c'}$
$\frac{V_{EXP.}}{f_c'}$
4
5
6
7
8
9
10
11
DOWEL DIAMETER (1/8 INCH)

FIG. 5.66

plot of equation 5-2. Due to varying concrete strengths and hence varying f_r, the graph of equation 5-2 is not a smooth and constantly increasing curve.

In Fig. 5.6b, equation 5-2 and the data points have been normalized. Each value of Fig. 5.6a has been divided by the corresponding concrete strength f_c^1 for that particular case (Table 5.2b). Both analytical and experimental curves exhibit similar shapes.

This model is reasonably accurate up to the #8 dowel size and begins to deviate substantially for the larger dowels. The cantilever model requires that the end condition be fixed, i.e., a fixed condition at the first stirrup location. This condition holds for the smaller dowels where the first stirrup does not yield and bending occurs in the top dowel within the 1" cantilever distance. On the other hand, the large dowels simply will not bend in a 1" distance and hence tend to yield the first stirrup in direct tension. Thus the fixed condition at the first stirrup would not hold true.

The above model does not take into account any direct tensile stresses or the effect of yielding of the first stirrup. These two points will be considered now.

The first visible sign of any cracking in the top dowel tests was as shown in Fig. 5.7, where a longitudinal crack propagated from the top dowel out towards the beam sides and then horizontally along the beam. The area over which direct tension occurs is a rectangle 6" (beam width) by 1" (distance to first stirrup), i.e., 6 square inches. With the tensile strength of

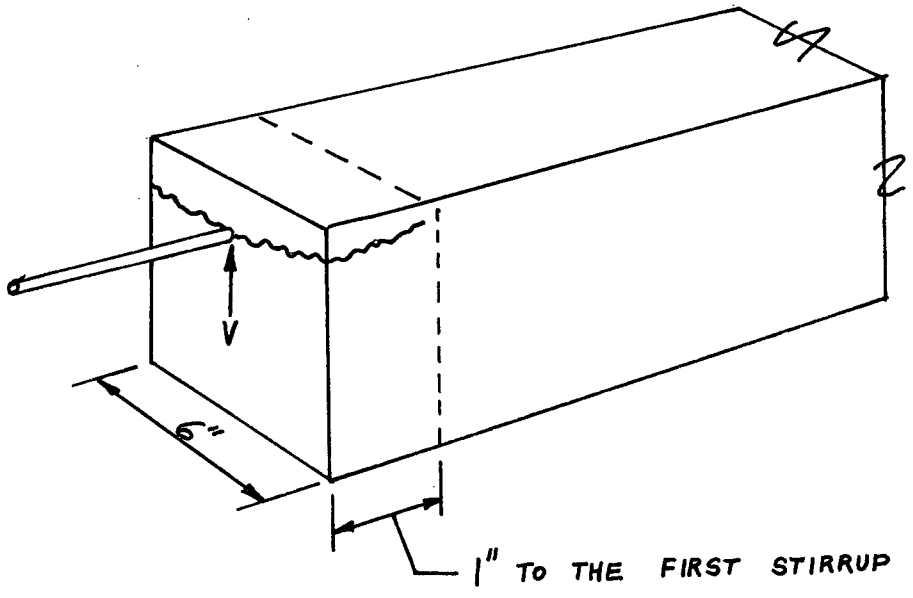

Fig. 5.7 Crack Propagation in Top Dowel Test

concrete taken as $7.5\sqrt{f'_c}$, the shear force required to crack the section can be calculated directly as

$$V = 7.5\sqrt{f'_c} * 6 \qquad (5\text{-}3)$$

The results of this calculation are listed in Table 5.3 and Fig. 5.9 shows a plot of equation 5-3 in relation to other experimental values.

The effect of the first stirrup yielding shall be considered next. Fig. 5.8 illustrates the condition at the first stirrup where the shear force V is resisted by the tension in the stirrup. The values given in Table 5.4 are plotted in Fig. 5.9 as two discontinuous straight lines (stirrup sizes #3 and #4). These two lines agree reasonably well with the ultimate values obtained from experiment.

In this test series, it was difficult to compare the experimental and model deflections. Since the first stirrup will strain and therefore extend under the application of load, the deflection that is measured at positions 1 (or 2) is not identically the same as the deflection of the top dowel vertically above position 1 (or 2). (Refer to Fig. 5.2.)

As shown in Fig. 5.9, the ultimate shear is considerably higher than that obtained at 0.03" deflection. The #4 dowel failed in shear at ultimate (Fig. 5.10). In the case of #7 and #8 dowels, the first stirrup ruptured at ultimate (Fig. 5.11). The #9, #10 and #11 test specimens had #4 size stirrups and in these three cases the concrete beam failed in shear (at the end with the larger stirrup spacing - Fig. 5.13).

Table 5.3 Direct Tensile Force

Dowel Size	$f_r = 7.5\sqrt{f'_c}$ (Ksi)	$V = 7.5\sqrt{f'_c} * 6$ (KIPS)
#4	0.565	3.39
#5	0.42	2.52
#6	0.42	2.52
#7	0.565	3.39
#8	0.42	2.52
#9	0.565	3.39
#10	0.565	3.39
#11	0.580	3.48

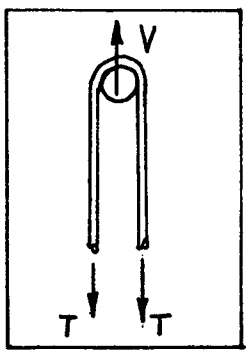

Fig. 5.8 Yielding of the First Stirrup

Table 5.4 Tension at Stirrup Yield

Dowel Size	Stirrup Size	A_s Stirrup Area $(in.^2)$	f_y (Ksi)	$2T = A_s f_y$ KIPS
#4	#3	0.22	54	11.88
#5				
#6				
#7				
#8				
#9	#4	0.40	60	24
#10				
#11				

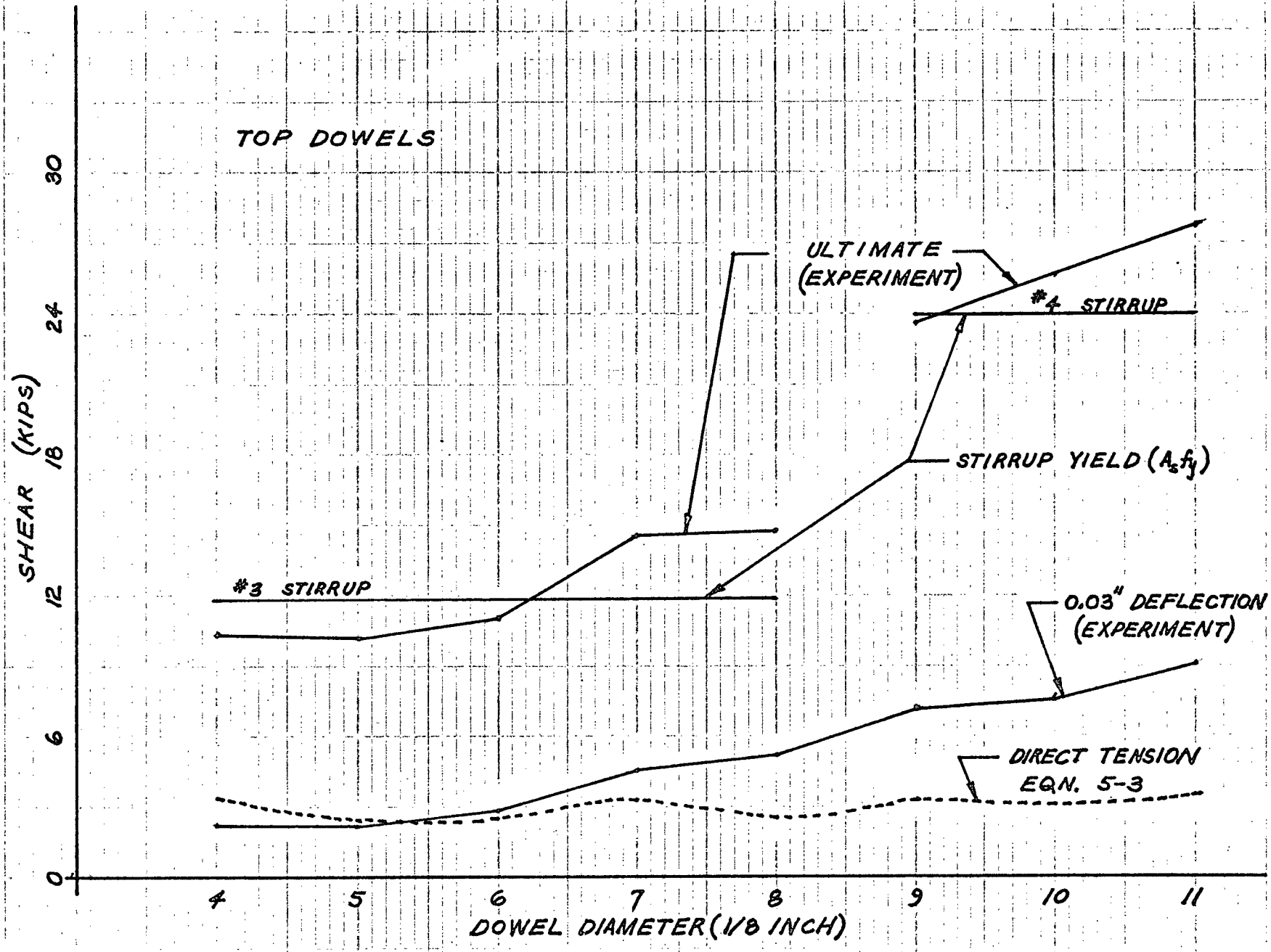
TOP DOWELS
SHEAR (KIPS)
0
6
12
18
24
30
ULTIMATE (EXPERIMENT)
#4 STIRRUP
STIRRUP YIELD ($A_s f_y$)
#3 STIRRUP
0.03" DEFLECTION (EXPERIMENT)
DIRECT TENSION EQN. 5-3
4
5
6
7
8
9
10
11
DOWEL DIAMETER (1/8 INCH)

FIG. 5.9

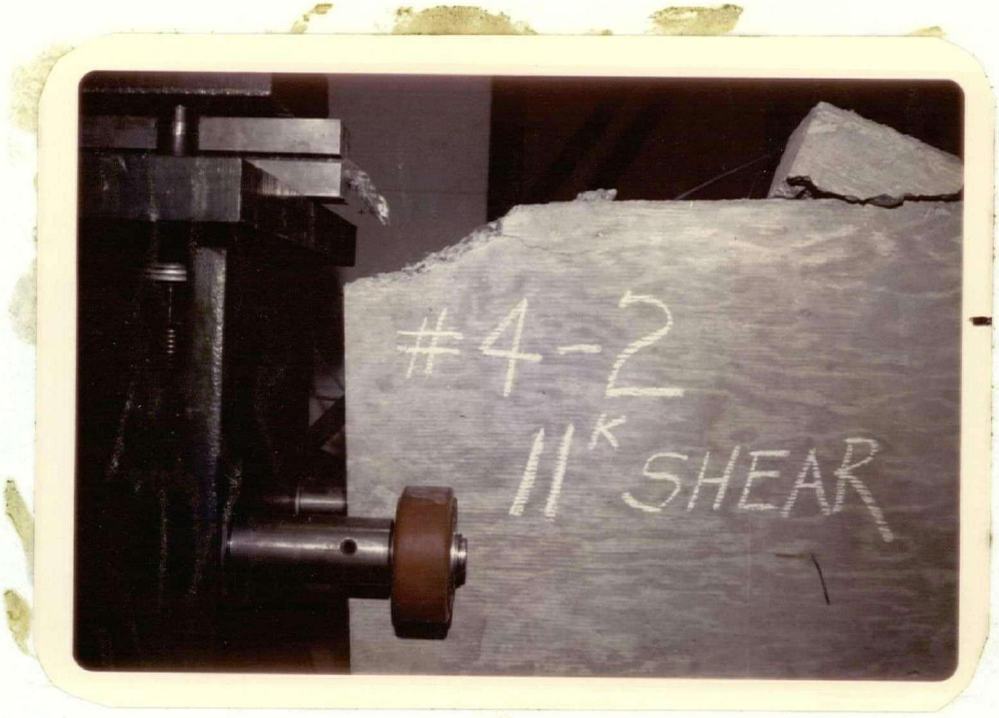

Fig. 5.10 Shear Failure of #4 Dowel

Fig. 5.11 Rupture of First Stirrup

Fig. 5.12 Crack Pattern in Top Dowel Test

Fig. 5.13 Specimen at Ultimate Load

Even though the stirrup spacing was varied on both halves of the test beams, no significant differences in the behaviour or cracking patterns was observed between the two ends. Figs. 5.12 and 5.13 show the crack patterns during testing and at ultimate load.

CHAPTER 6. THE JOINT:SUM OF TOP AND BOTTOM DOWELS

The previous two chapters have discussed bottom and top dowel tests and analysis. In this chapter the results are combined and the shear capacity of a beam-column joint is calculated.

The graphs in Fig. 6.1 are the theoretical values obtained previously, plotted for the same deflection (0.03 in.) for both bottom and top dowels. As can be noted from the graphs, the bottom dowels contribute most to the shear capacity of a joint. In nearly all cases, the shear for a top dowel is between 33 - 44% of that for the same size bottom dowel. For the bottom dowel curve, the value for the foundation modulus K (and hence β) corresponds to a concrete strength of f'_c equal to 4,000 psi. Similarly, the modulus of rupture f_r is calculated for the same concrete strength and equation 5-2 plotted.

The joint shown in Fig. 6.2 could be considered as a design problem. All the shear is to be transferred by dowel action and hence the shear capacity of this joint can be calculated by using the graphs presented in Fig. 6.1. In determining the shear capacity of the bottom dowels in this case, the expression $P = 2\beta^3 EIy$ is used. The bending moment term βM is neglected in this case because it is extremely doubtful that the plastic bending moment could be developed in the bottom dowels at the beam-column interface.

The deflection of the bottom dowels is symmetric about the beam-column interface with the point of inflection occurring at the beam-column interface.

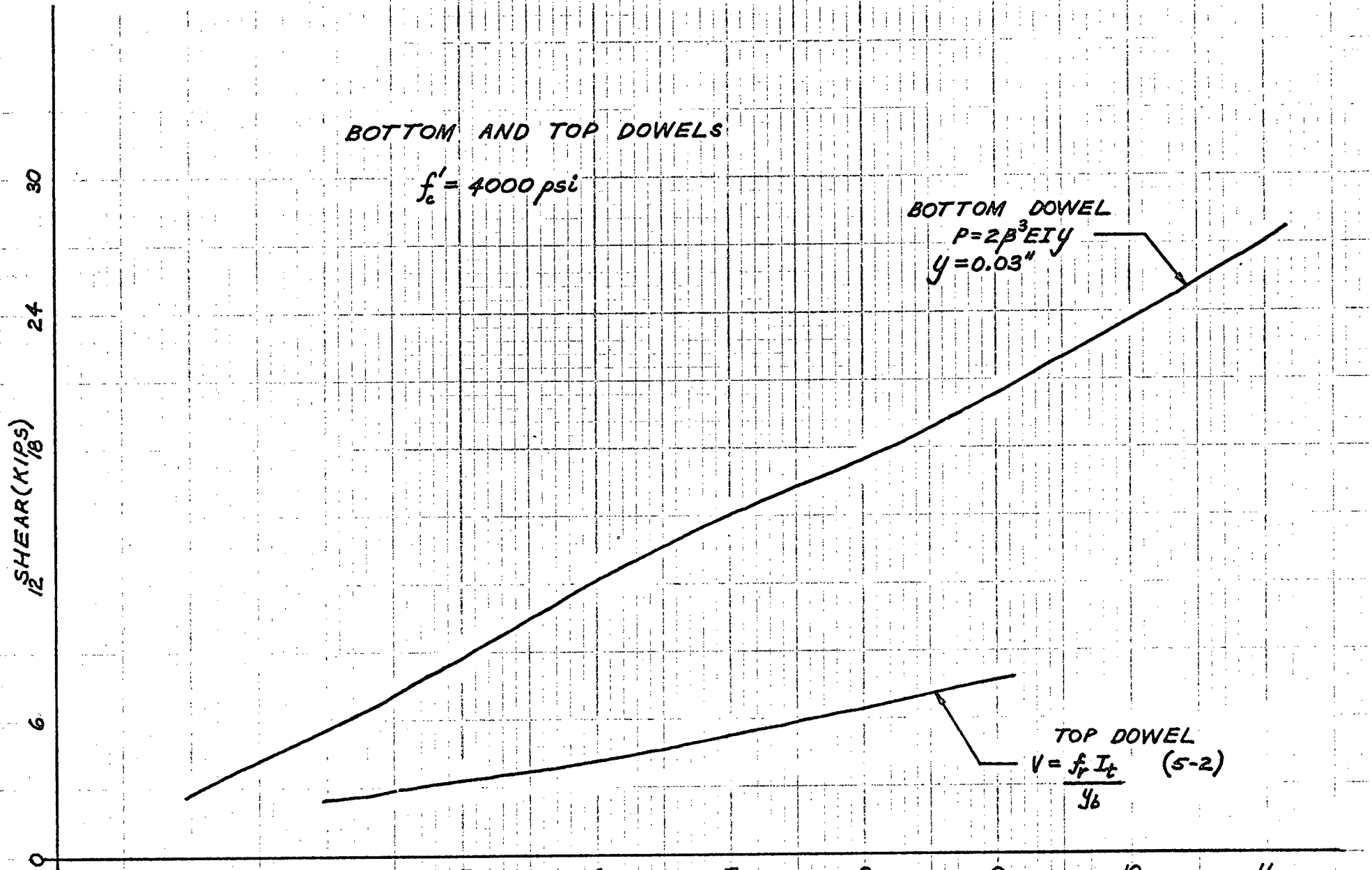
BOTTOM AND TOP DOWELS
$f_c' = 4000$ psi
BOTTOM DOWEL
$P = 2\beta^3 EIy$
$y = 0.03''$
TOP DOWEL
$V = \frac{f_r I_t}{y_b}$ (5-2)
SHEAR ($\frac{12}{18}$ KIPS)
0
6
24
30
3
4
5
6
7
8
9
10
11
DOWEL DIAMETER (1/8 INCH)

FIG. 6.1

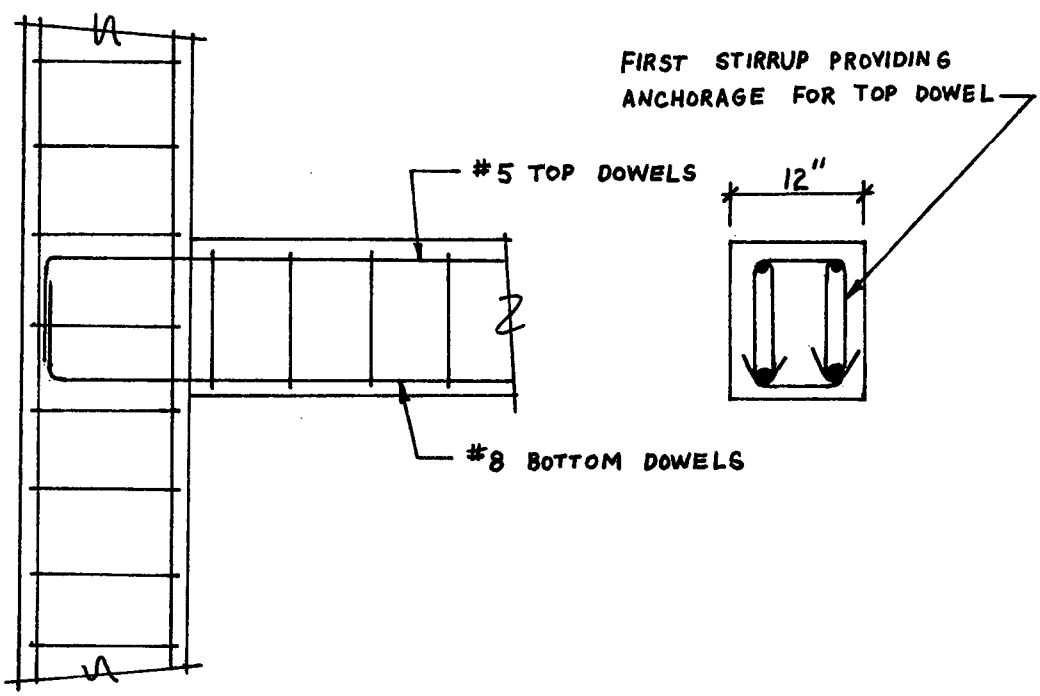

Fig. 6.2 Design Beam-Column Joint

From the graphs of Fig. 6.1:

Bottom Dowel shear:	2 x 17.4	=	34.8^k
Top Dowel shear:	2 x 3.0	=	6.0^k
	Total		40.8^k

The shear capacity of this joint, assuming dowel action only, is 40 kips (service load shear).

As shown in Fig. 6.2, the first stirrup should be placed around each top dowel individually. This provides the necessary tie-down force to the top dowels and hence a greater contribution to the shear capacity. As was mentioned before, the shear capacity of the top dowels is sensitive to the distance to the first stirrup. Also, since the deflection of the bottom dowels is assumed to be symmetrical about the beam-column interface, the net beam deflection would be 0.03 + 0.03 = 0.06" at a shear force of 40 kips. At such small deflections, the stress pattern around one dowel is assumed not to influence the behaviour of its neighbouring dowel. Hence the shear capacity of the dowels is assumed to be additive directly. At large deflections, the interaction and overlapping of stress patterns between neighbouring dowels may be significant. Therefore the ultimate shear capacities would not be additive directly.

This analysis has neglected the effect of friction and bending moment at the beam-column interface. These effects, however, will only help to increase the shear capacity of the joint and therefore a design based only on the dowel action of the reinforcing bars provides a lower bound on the joint capacity.

Fig. 6.3 shows the relative positions of the graphs for ultimate shear for both top and bottom dowels. These graphs, however, can not be used to accurately predict the ultimate shear capacity for a combination of top and bottom dowels because of interactive stress effects between dowels.

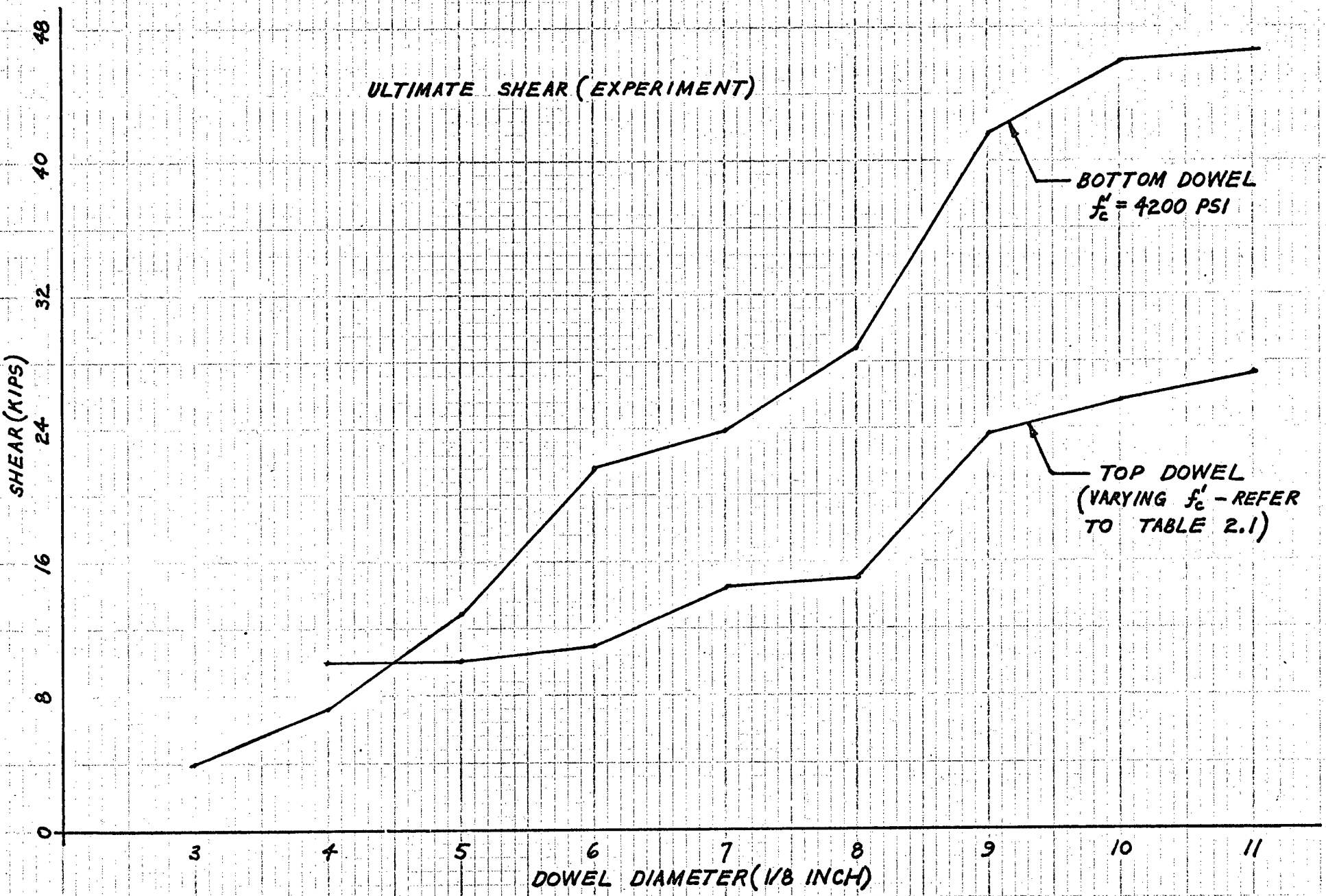
ULTIMATE SHEAR (EXPERIMENT)
BOTTOM DOWEL
f'_c = 4200 PSI
TOP DOWEL
(VARYING f'_c - REFER
TO TABLE 2.1)
SHEAR (KIPS)
0
8
16
24
32
40
48
3
4
5
6
7
8
9
10
11
DOWEL DIAMETER (1/8 INCH)

FIG. 6.3

CHAPTER 7. CONCLUSIONS

1. The beam-on-elastic foundation analogy forms a reasonable method of modelling the behaviour of the bottom dowel and its applicability could be confidently extrapolated to other situations which are not exactly the same as those presented here.

2. The beam-on-elastic foundation model should not be extrapolated to large values of deflection; 0.03" deflection is a recommended upper limit.

3. A beam column joint designed solely on the basis of dowel action of the reinforcing steel bars may provide adequate shear capacity.

4. The bottom dowels are the major shear-carrying components of a beam-column joint.

5. The top dowel should be well anchored by the first stirrup if it is to contribute to the shear capacity of the joint.

6. The variation of stirrup spacing in the beam specimens did not have any effect on the shear capacity of the top dowels.

7. There is a wide range of values for the foundation modulus between the small and large dowels - 200 to 1,000 Ksi.

REFERENCES

1. Peter, B.G.W., M.A.Sc. Thesis, University of British Columbia, Vancouver, 1971.

2. Mast, R. F., "Auxiliary Reinforcement in Concrete Connections", J. Str. Div. ASCE, June 1968, pp. 1485-1503.

3. Hofbeck, J. A., Ibrahim, I.O., and Mattock, Alan H., "Shear Transfer in Reinforced Concrete", ACI Journal, February 1969, pp. 119-128.

4. Hanson, Norman W. and Connor, Harold W., "Seismic Resistance of Reinforced Concrete Beam-Column Joints", J. Str. Div. ASCE, October 1967, pp. 533-560.

5. Timoshenko, S., "Strength of Materials - Part II", Princeton, N.J., D. Van Nostrand Company Inc., March 1956.

6. Birkeland, Philip W. and Birkeland, Halvard W., "Connections in Precast Concrete Construction", ACI Journal, March 1966, pp. 345-368.

7. Kriz, L. B. and Raths, C. H., "Connections in Precast Concrete Structures - Strength of Corbels", PCI Journal, February 1965, pp. 16-61.

8. Gaston, J. R. and Kriz, L. B., "Connections in Precast Concrete Structures - Scarf Joints", PCI Journal, June 1964, pp. 37-59.

9. ACI-ASCE Committee 512, "Suggested Design of Joints and Connections in Precast Structural Concrete", ACI Journal,

August 1964, pp. 921-937.

10. Prestressed Concrete Institute, "PCI Design Handbook Precast and Prestressed Concrete", Chicago, Illinois, 1971.

11. Kratz, R. D., M.A.Sc. Thesis, University of British Columbia, Vancouver, 1970.

12. Dulacska, Helen, "Dowel Action of Reinforcement Crossing Cracks in Concrete", ACI Journal, December 1972, pp. 754-757.

13. Anderson, Arthur R., "Composite Designs in Precast and Cast-in-Place Concrete", Progressive Architecture, September 1960, pp. 172-179.

APPENDIX 1. BOTTOM DOWEL EXPERIMENTAL GRAPHS

The following graphs are the experimental shear-deflection results for the bottom dowel tests. Each graph is labelled according to the notation used in Fig. 4.2 in Chapter 4.

For example, a curve labelled as 1-A indicates the deflection at position 1 of test series A.

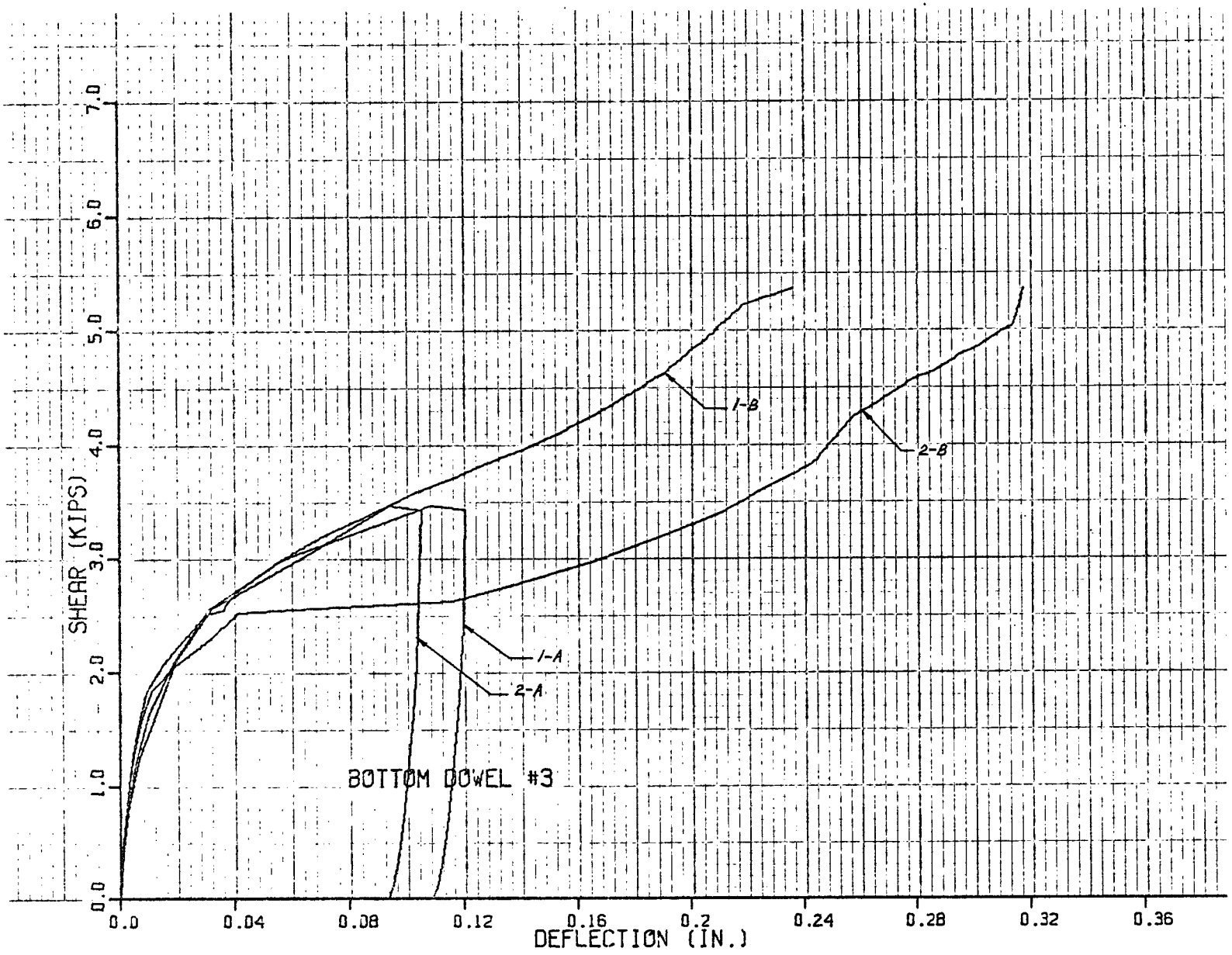
SHEAR (KIPS)
0.0
1.0
2.0
3.0
4.0
5.0
6.0
7.0
0.0
0.04
0.08
0.12
0.16
0.2
0.24
0.28
0.32
0.36
DEFLECTION (IN.)
1-B
2-B
1-A
2-A
BOTTOM DOWEL #3

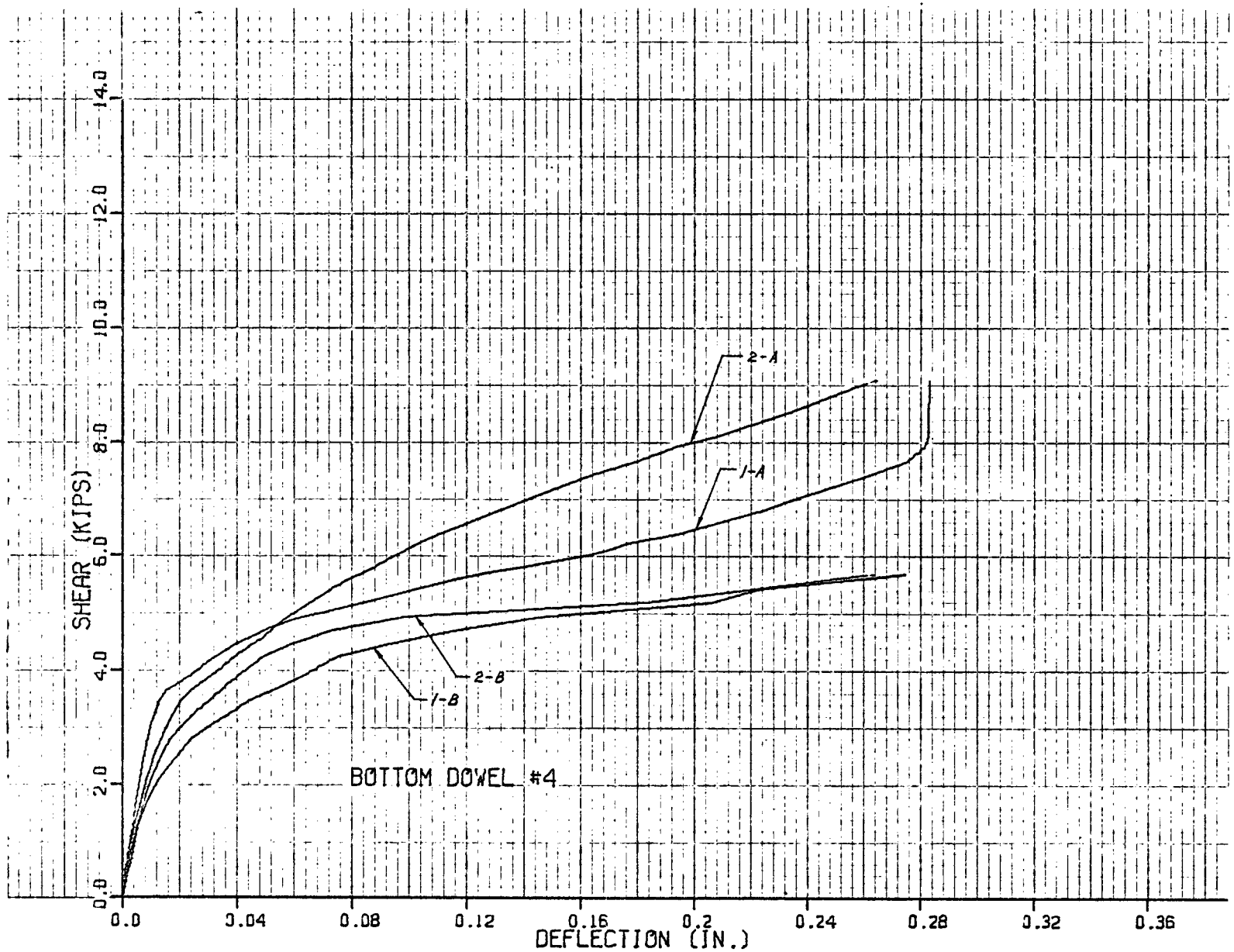
SHEAR (KIPS)
0.0
2.0
4.0
6.0
8.0
10.0
12.0
14.0
0.0
0.04
0.08
0.12
0.16
0.2
0.24
0.28
0.32
0.36
DEFLECTION (IN.)
2-A
1-A
2-B
1-B
BOTTOM DOWEL #4

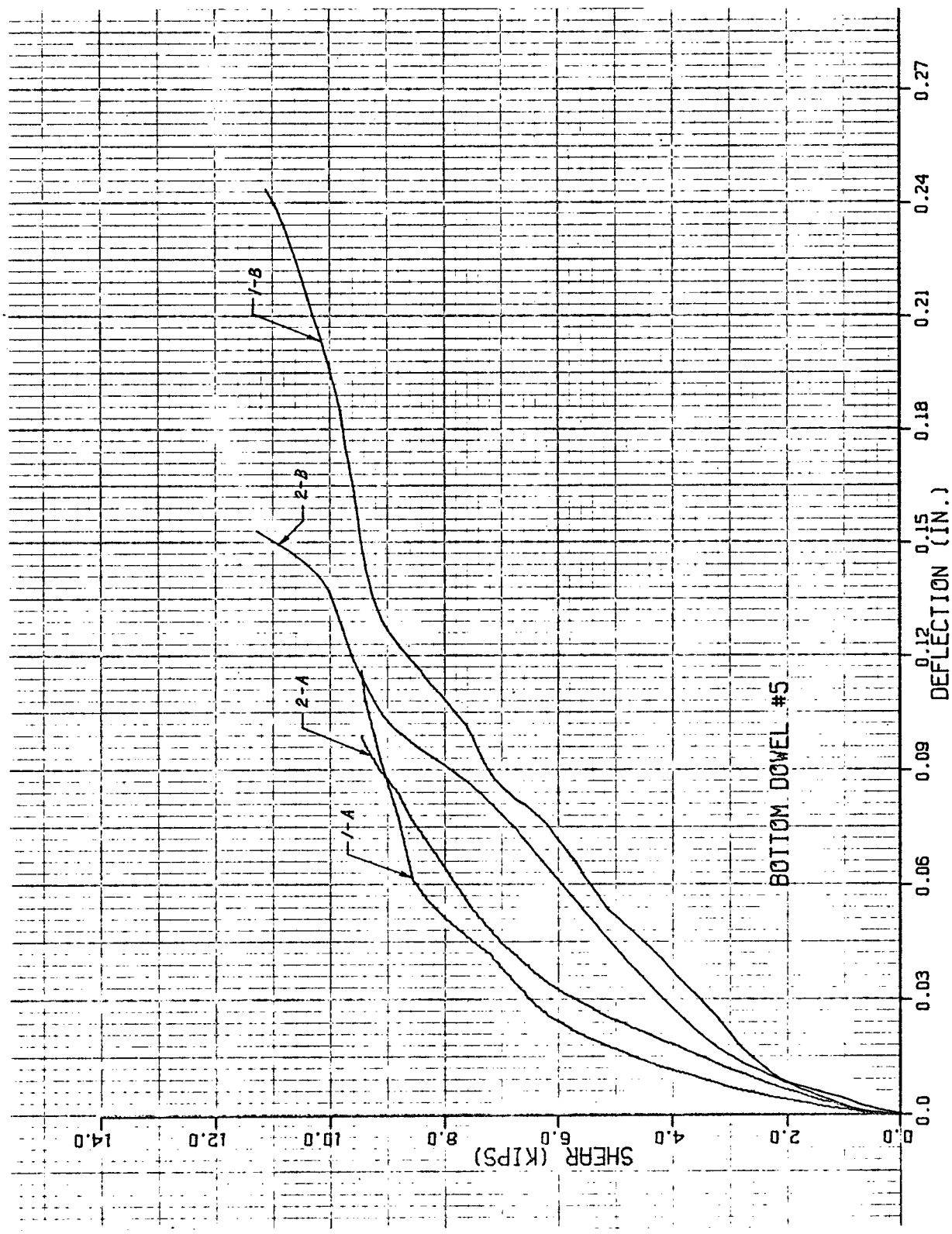
BOTTOM DOWEL #5
SHEAR (KIPS)
DEFLECTION (IN.)
0.0
2.0
4.0
6.0
8.0
10.0
12.0
14.0
0.0
0.03
0.06
0.09
0.12
0.15
0.18
0.21
0.24
0.27
1-B
2-B
2-A
1-A

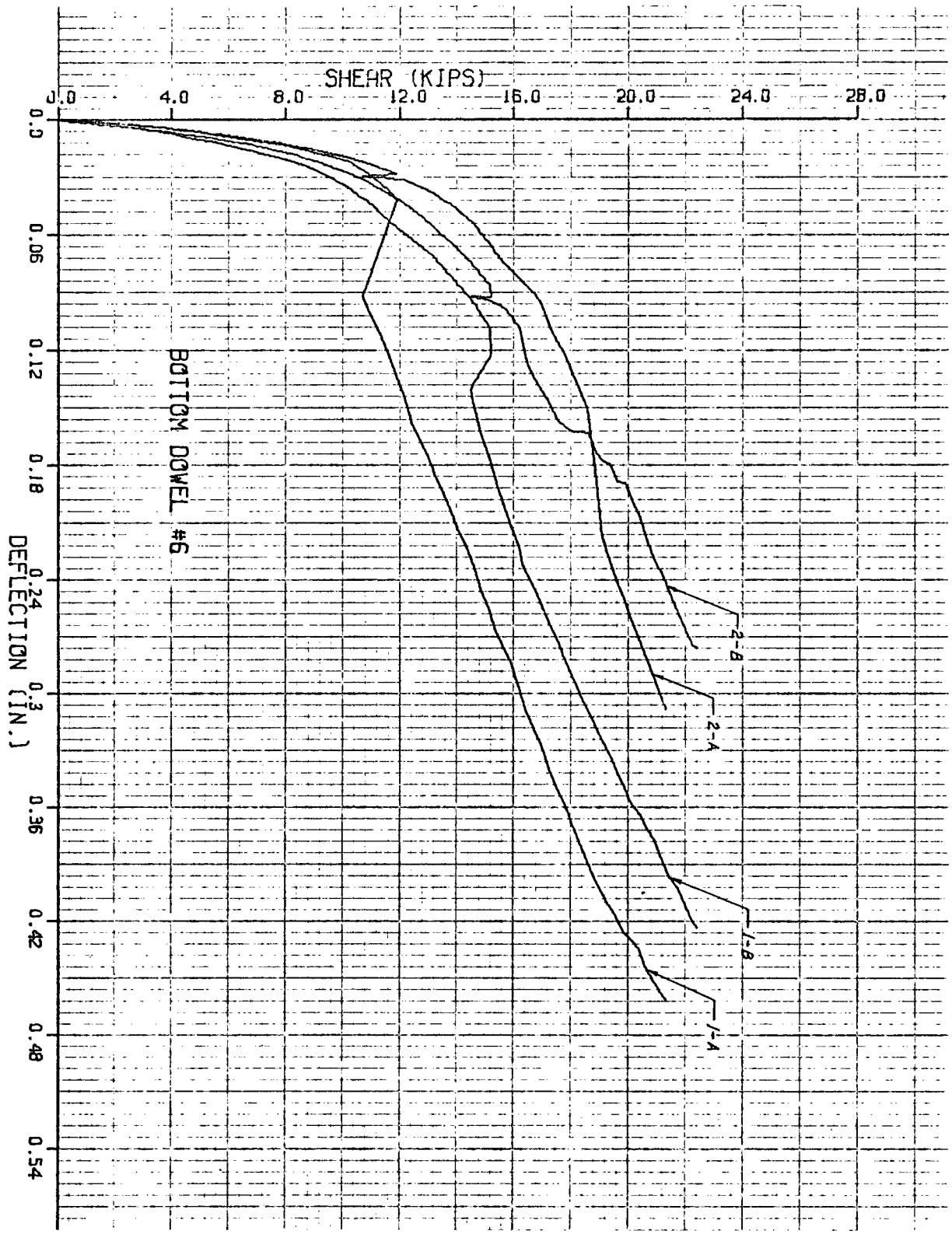
SHEAR (KIPS)
0.0
4.0
8.0
12.0
16.0
20.0
24.0
28.0
0.0
0.06
0.12
0.18
0.24
0.3
0.36
0.42
0.48
0.54
DEFLECTION (IN.)
BOTTOM DOWEL #6
2-B
2-A
1-B
1-A

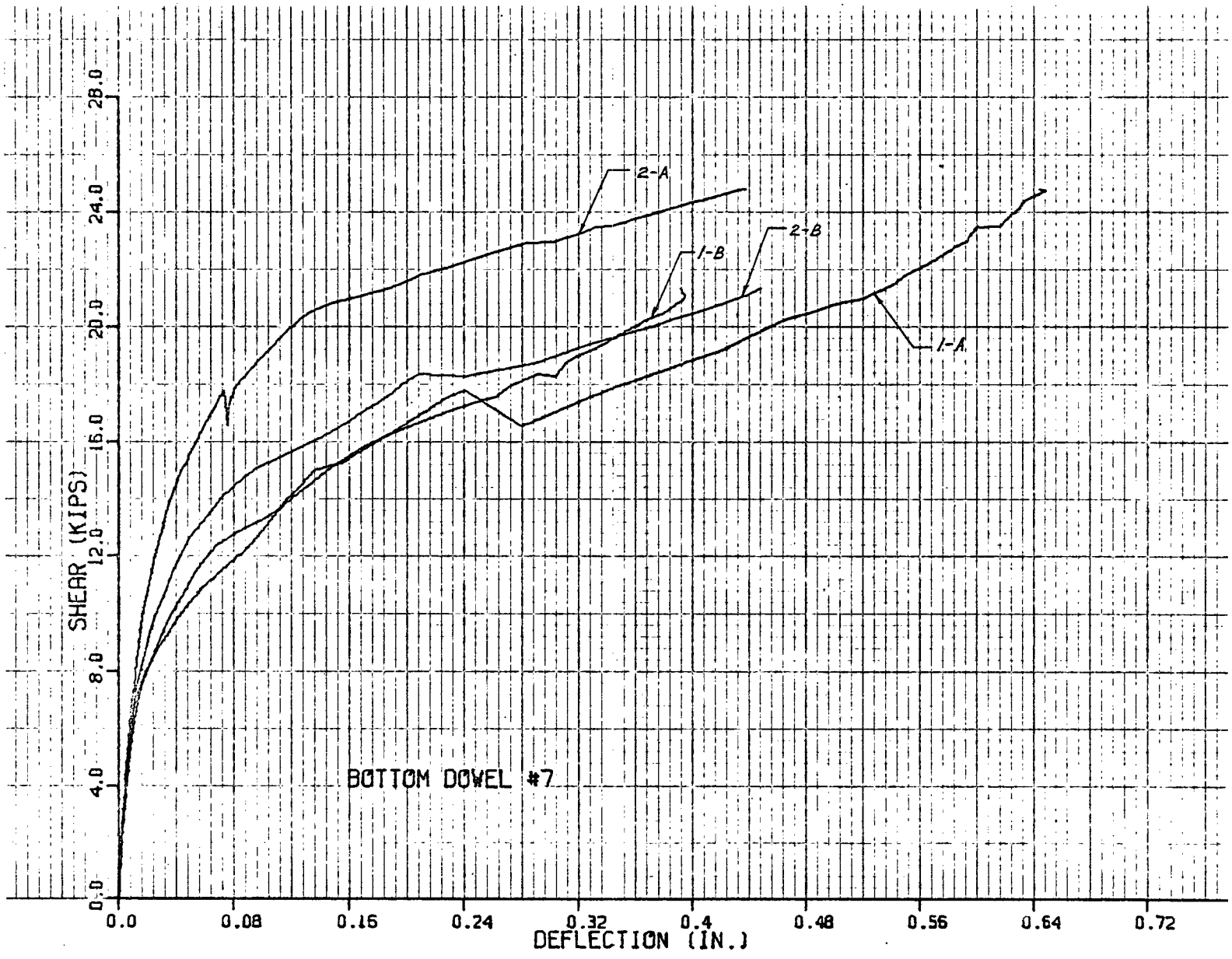
2-A
2-B
1-B
1-A
BOTTOM DOWEL #7
SHEAR (KIPS)
0.0
4.0
8.0
12.0
16.0
20.0
24.0
28.0
0.0
0.08
0.16
0.24
0.32
0.4
0.48
0.56
0.64
0.72
DEFLECTION (IN.)

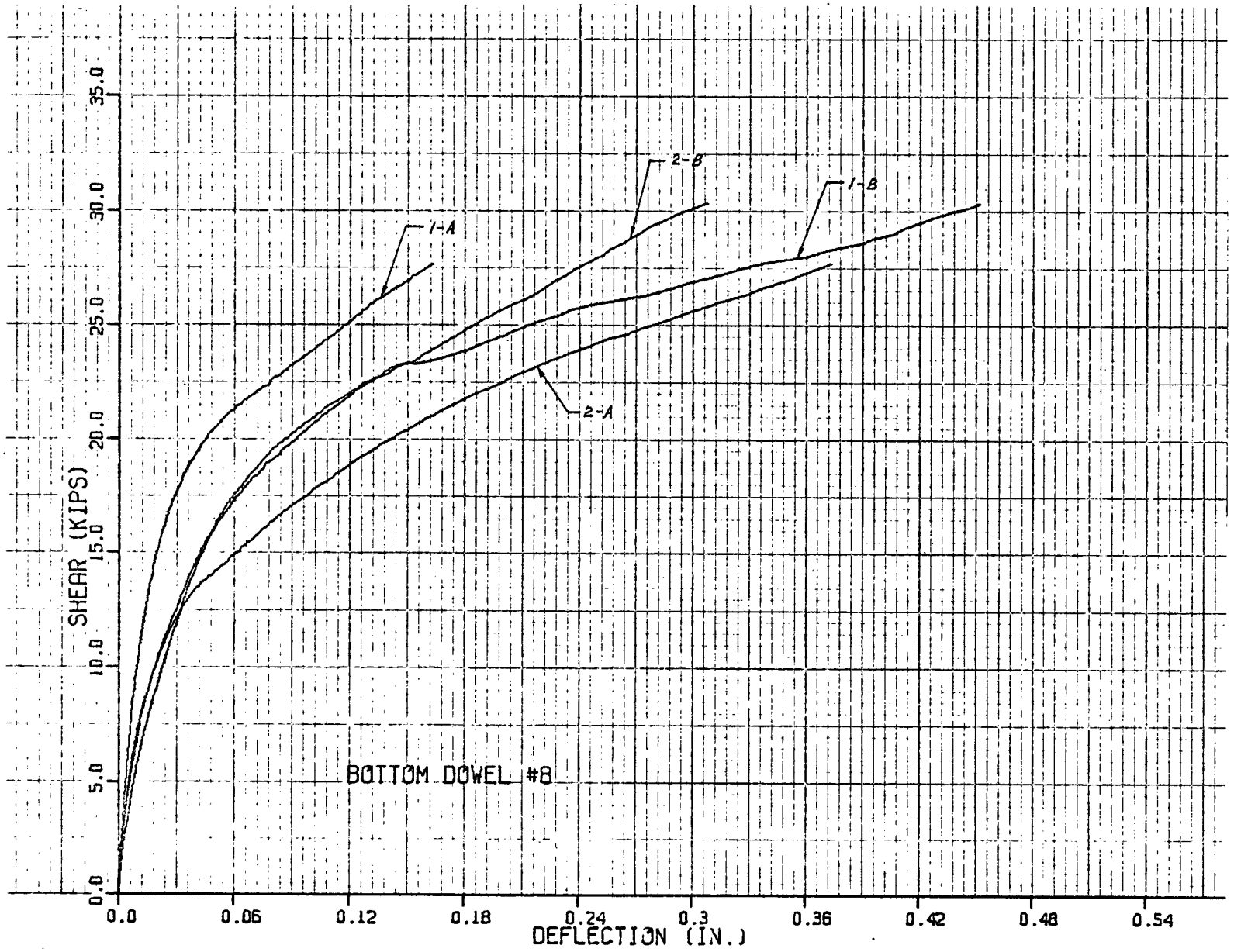
SHEAR (KIPS)
0.0
5.0
10.0
15.0
20.0
25.0
30.0
35.0
0.0
0.06
0.12
0.18
0.24
0.3
0.36
0.42
0.48
0.54
DEFLECTION (IN.)
1-A
2-B
1-B
2-A
BOTTOM DOWEL #8

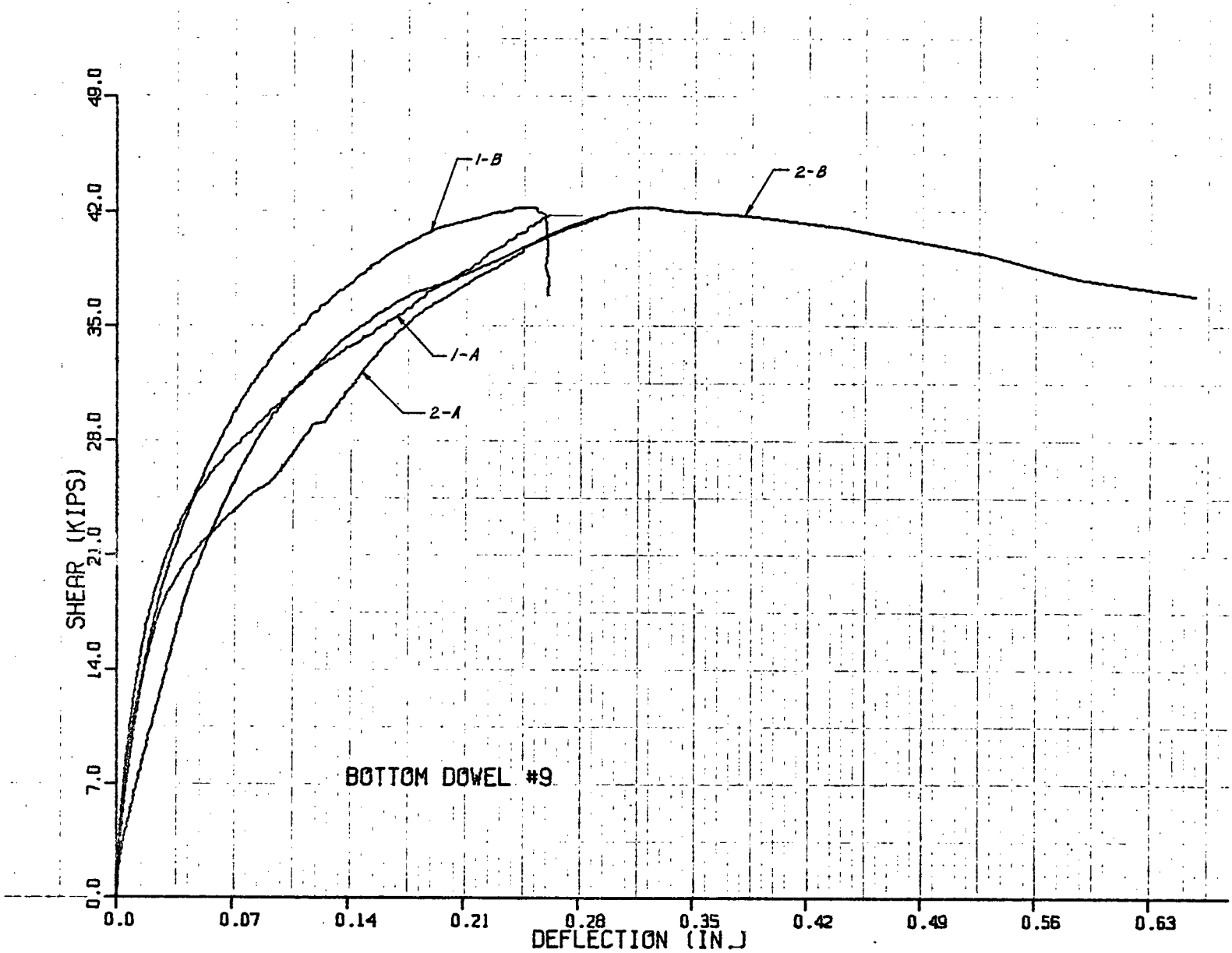
1-B
2-B
1-A
2-A
BOTTOM DOWEL #9
SHEAR (KIPS)
0.0
7.0
14.0
21.0
28.0
35.0
42.0
49.0
0.0
0.07
0.14
0.21
0.28
0.35
0.42
0.49
0.56
0.63
DEFLECTION (IN.)

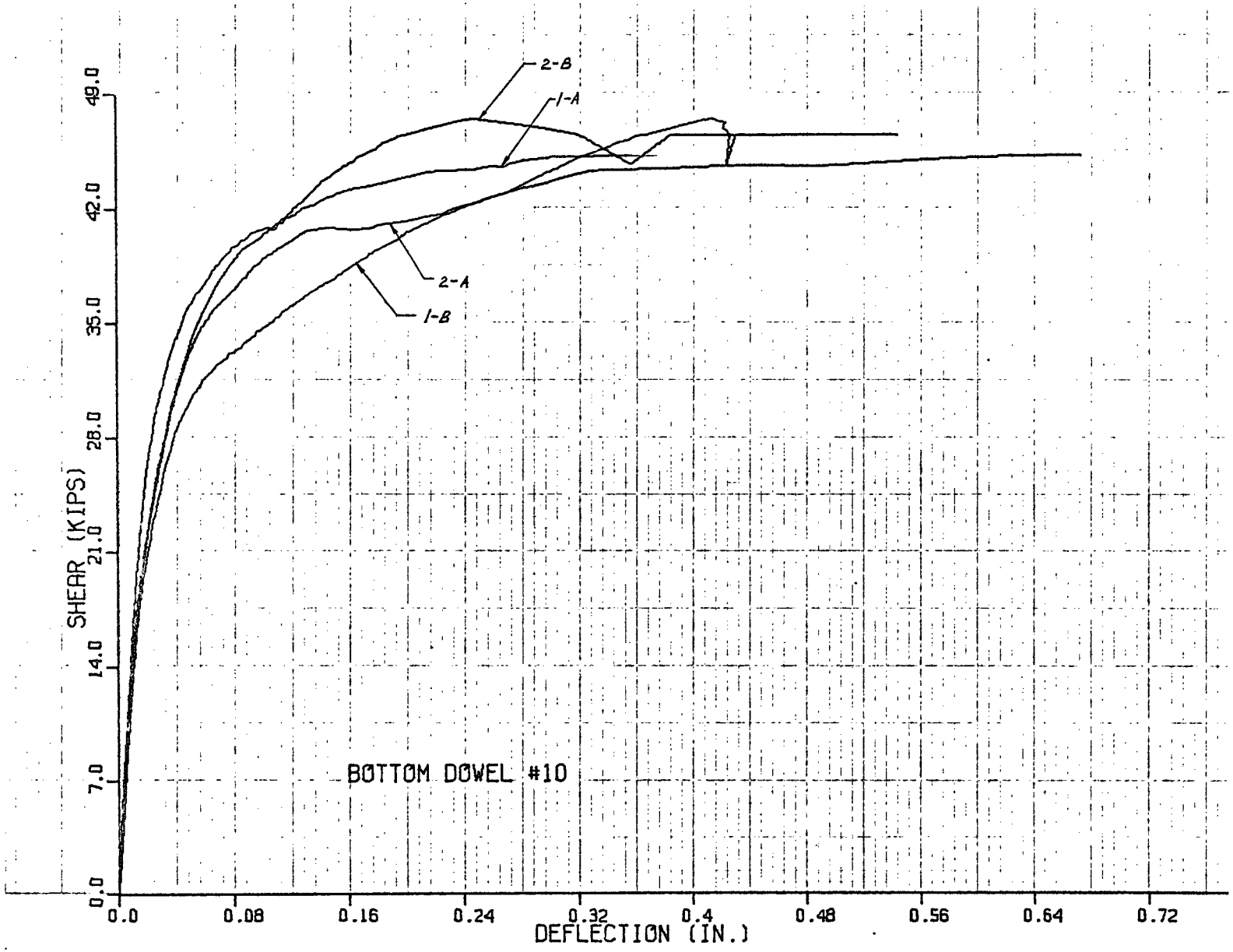
2-B
1-A
2-A
1-B
BOTTOM DOWEL #10
SHEAR (KIPS)
0.0
7.0
14.0
21.0
28.0
35.0
42.0
49.0
0.0
0.08
0.16
0.24
0.32
0.4
0.48
0.56
0.64
0.72
DEFLECTION (IN.)

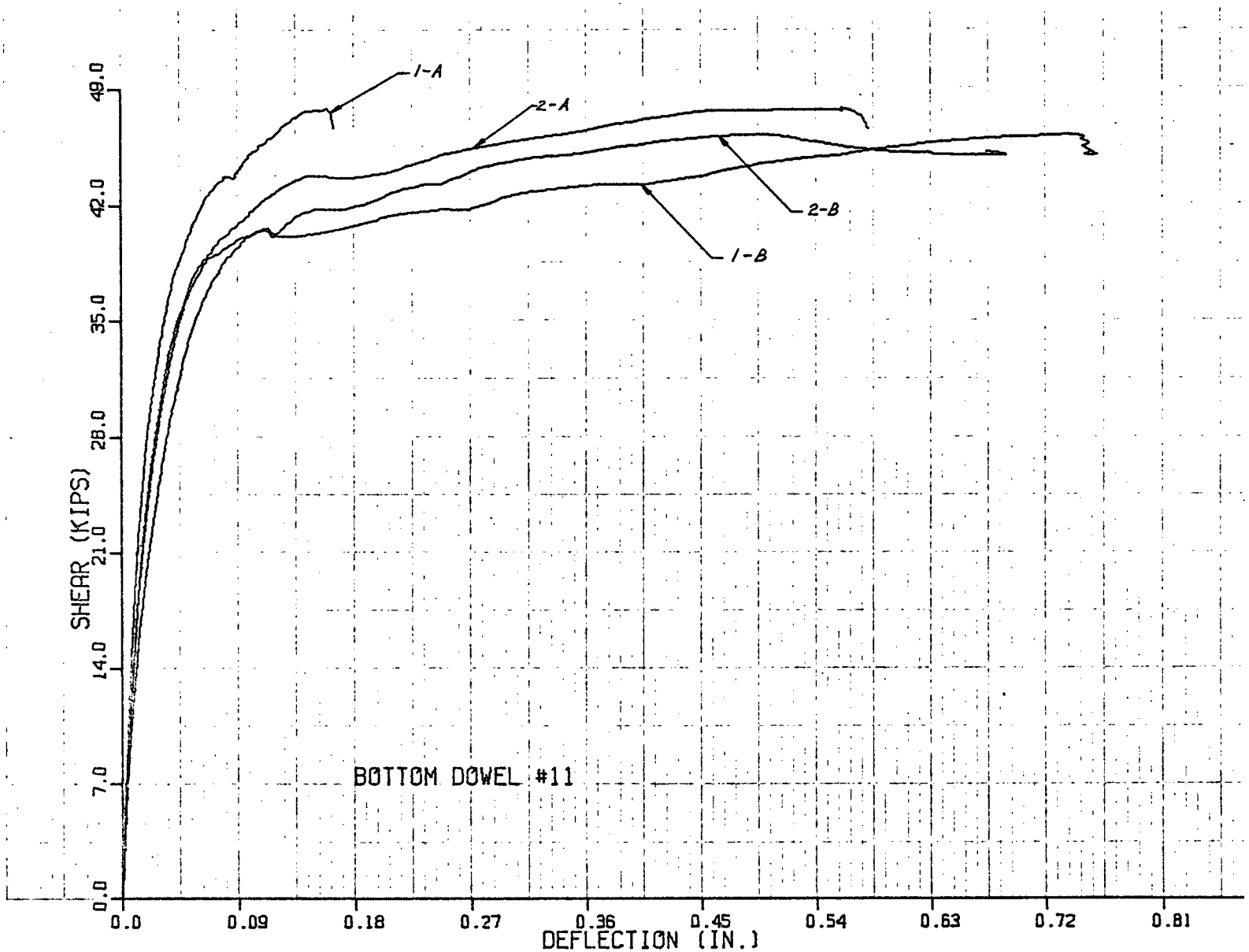
1-A
2-A
2-B
1-B
BOTTOM DOWEL #11
SHEAR (KIPS)
DEFLECTION (IN.)
0.0
7.0
14.0
21.0
28.0
35.0
42.0
49.0
0.0
0.09
0.18
0.27
0.36
0.45
0.54
0.63
0.72
0.81

APPENDIX 2. TOP DOWEL EXPERIMENTAL GRAPHS

The following graphs are the experimental shear-deflection results for the top dowel tests. Each graph is labelled according to the notation used in Fig. 5.2 in Chapter 5.

For example, a curve labelled as 1-A indicates the deflection at position 1 of test series A.

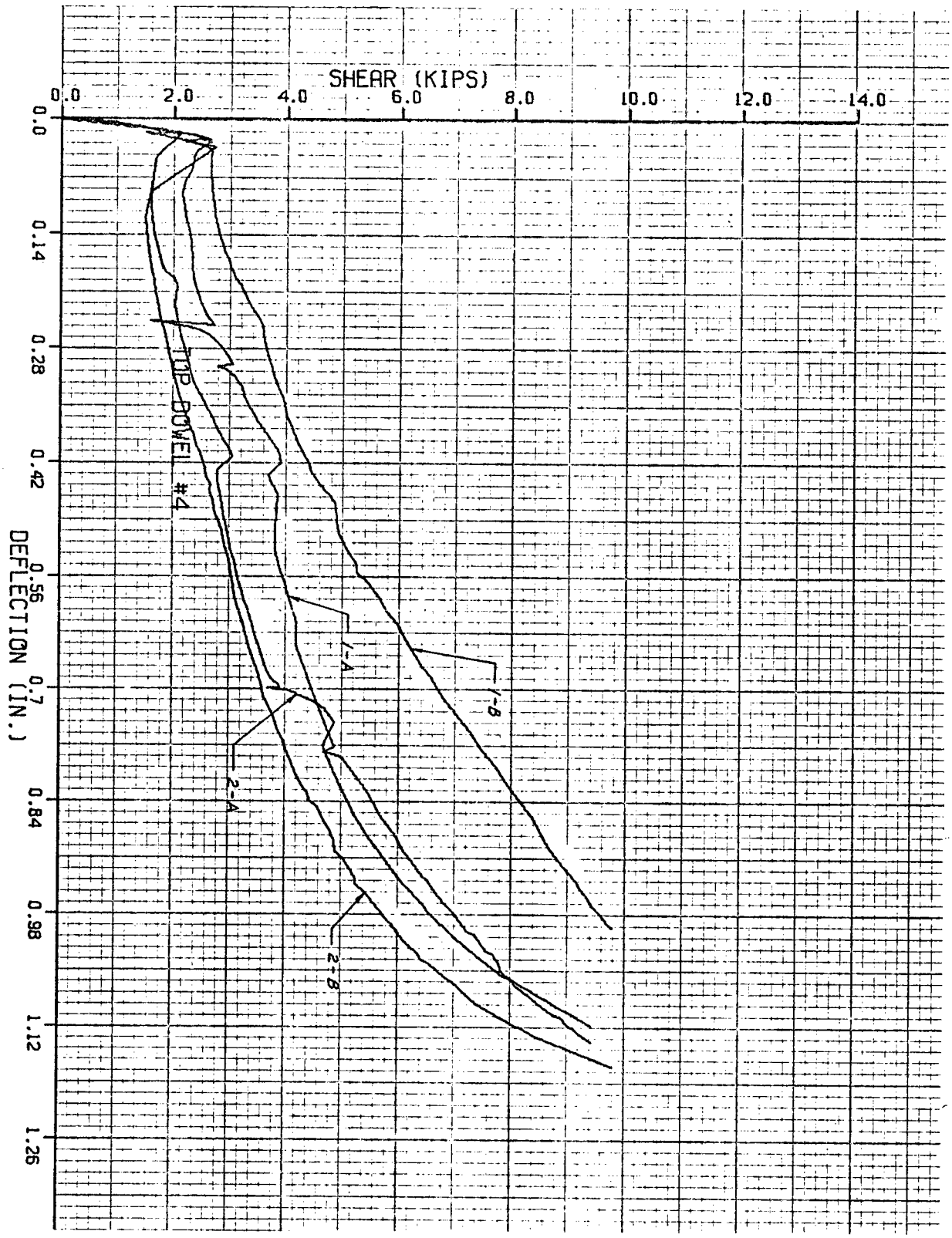
SHEAR (KIPS)
0.0
2.0
4.0
6.0
8.0
10.0
12.0
14.0
DEFLECTION (IN.)
0.0
0.14
0.28
0.42
0.56
0.7
0.84
0.98
1.12
1.26
TOP DOWEL #4
1-A
1-B
2-A
2-B

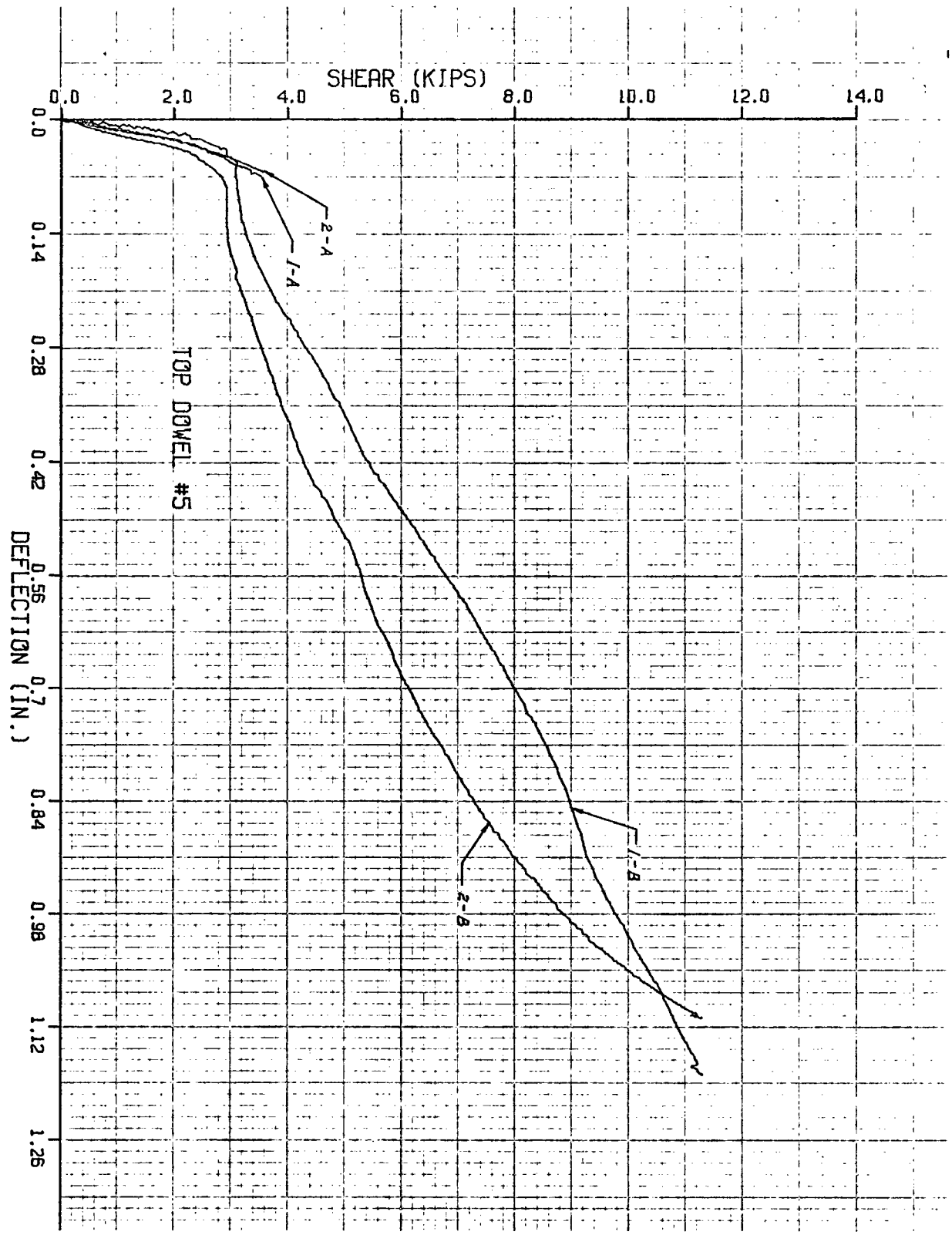
SHEAR (KIPS)
0.0
2.0
4.0
6.0
8.0
10.0
12.0
14.0
DEFLECTION (IN.)
0.0
0.14
0.28
0.42
0.56
0.7
0.84
0.98
1.12
1.26
TOP DOWEL #5
2-A
1-A
1-B
2-B

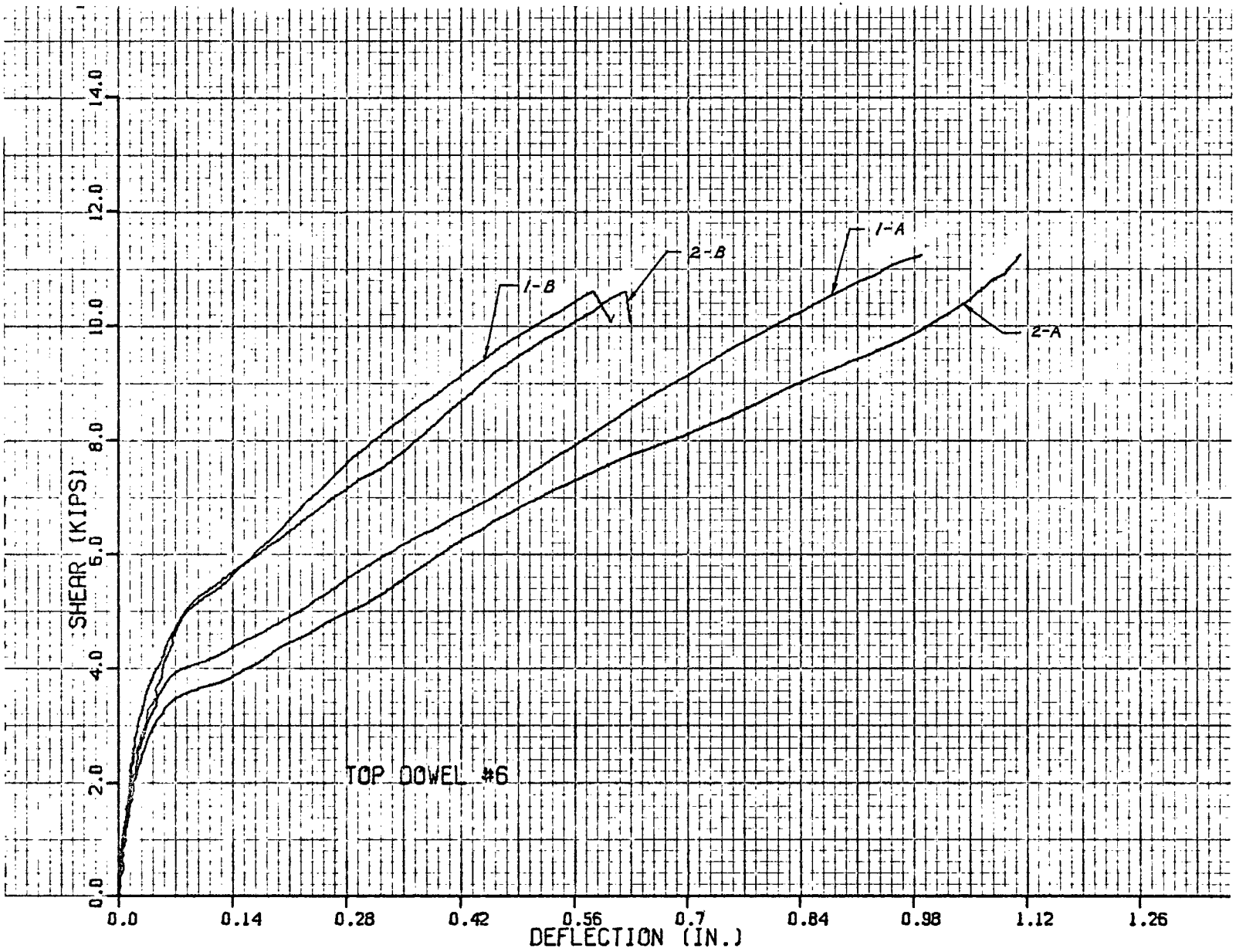
SHEAR (KIPS)
0.0
2.0
4.0
6.0
8.0
10.0
12.0
14.0
0.0
0.14
0.28
0.42
0.56
0.7
0.84
0.98
1.12
1.26
DEFLECTION (IN.)
1-A
2-B
1-B
2-A
TOP DOWEL #6

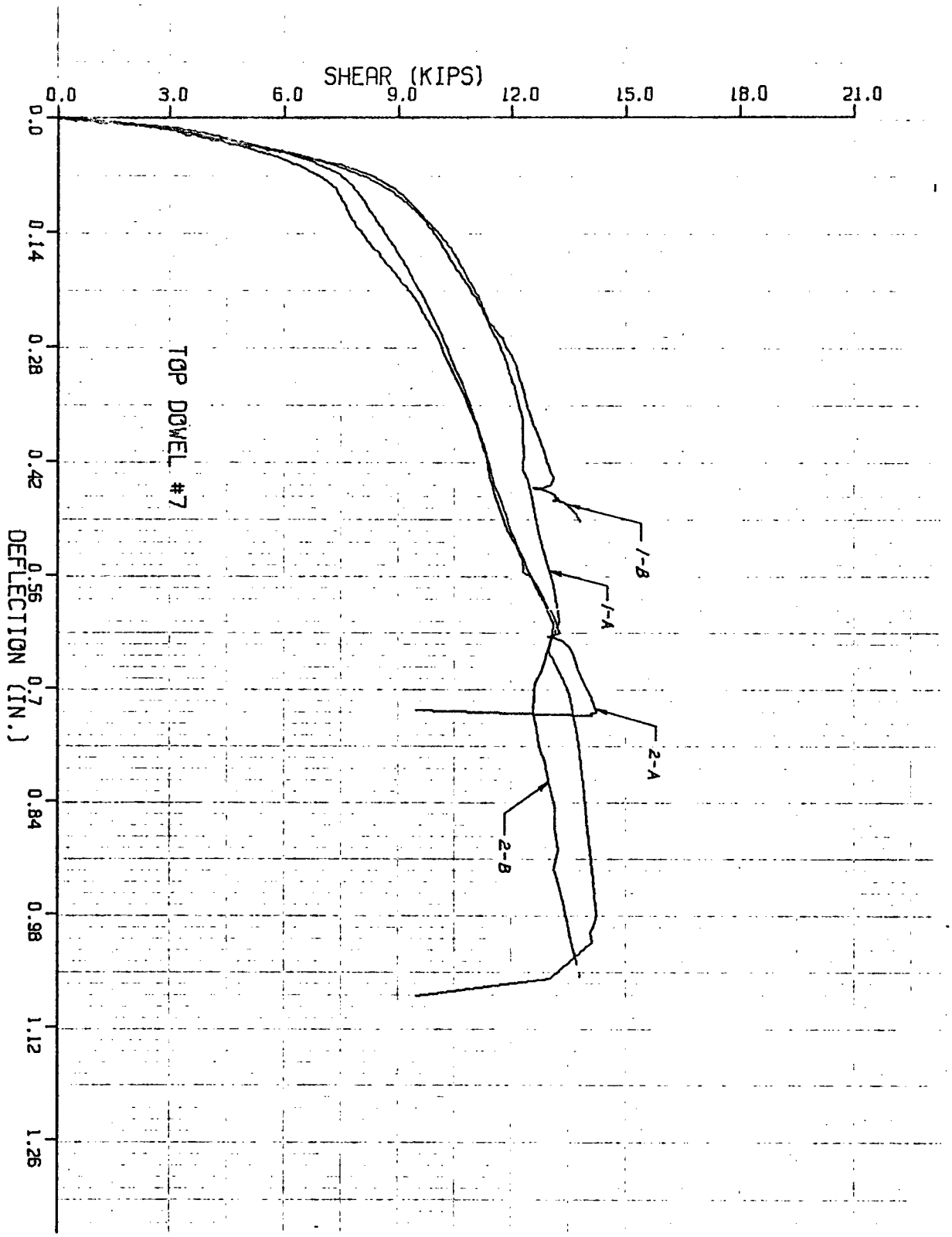
SHEAR (KIPS)
0.0
3.0
6.0
9.0
12.0
15.0
18.0
21.0
DEFLECTION (IN.)
0.0
0.14
0.28
0.42
0.56
0.7
0.84
0.98
1.12
1.26
TOP DOWEL #7
1-B
1-A
2-A
2-B

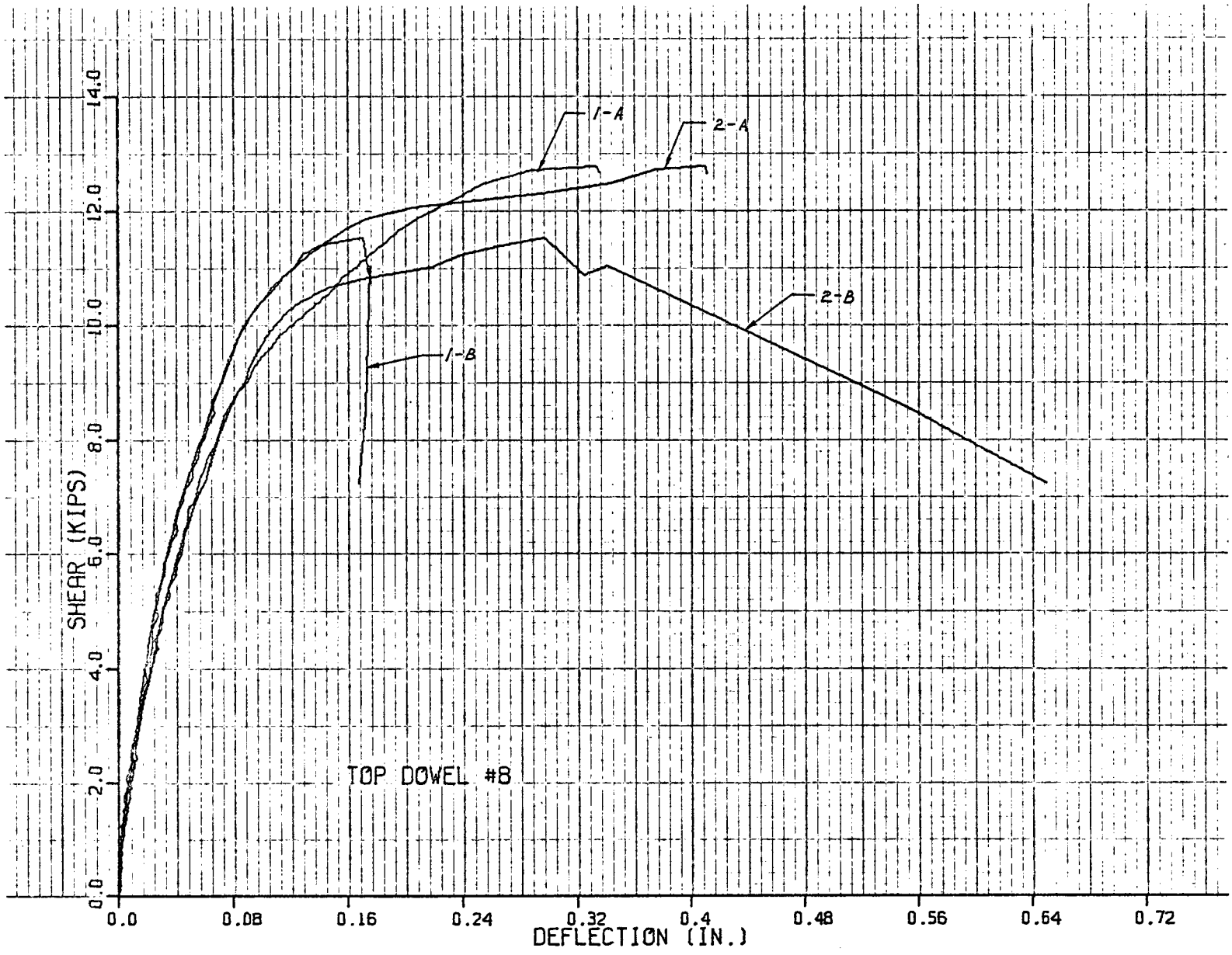
1-A
2-A
2-B
1-B
TOP DOWEL #8
SHEAR (KIPS)
0.0
2.0
4.0
6.0
8.0
10.0
12.0
14.0
0.0
0.08
0.16
0.24
0.32
0.4
0.48
0.56
0.64
0.72
DEFLECTION (IN.)

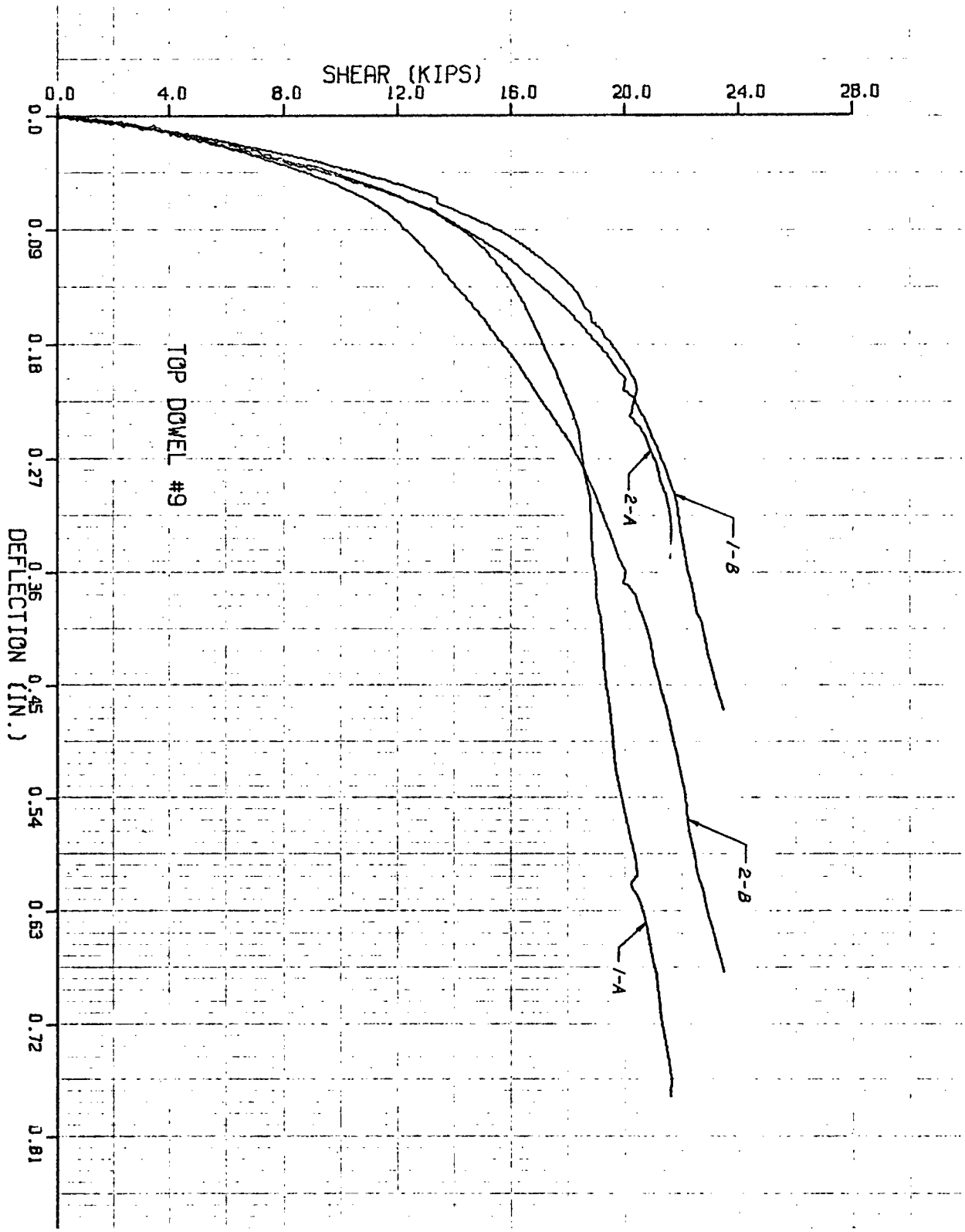
SHEAR (KIPS)
0.0
4.0
8.0
12.0
16.0
20.0
24.0
28.0
DEFLECTION (IN.)
0.0
0.09
0.18
0.27
0.36
0.45
0.54
0.63
0.72
0.81
TOP DOWEL #9
2-A
1-B
2-B
1-A

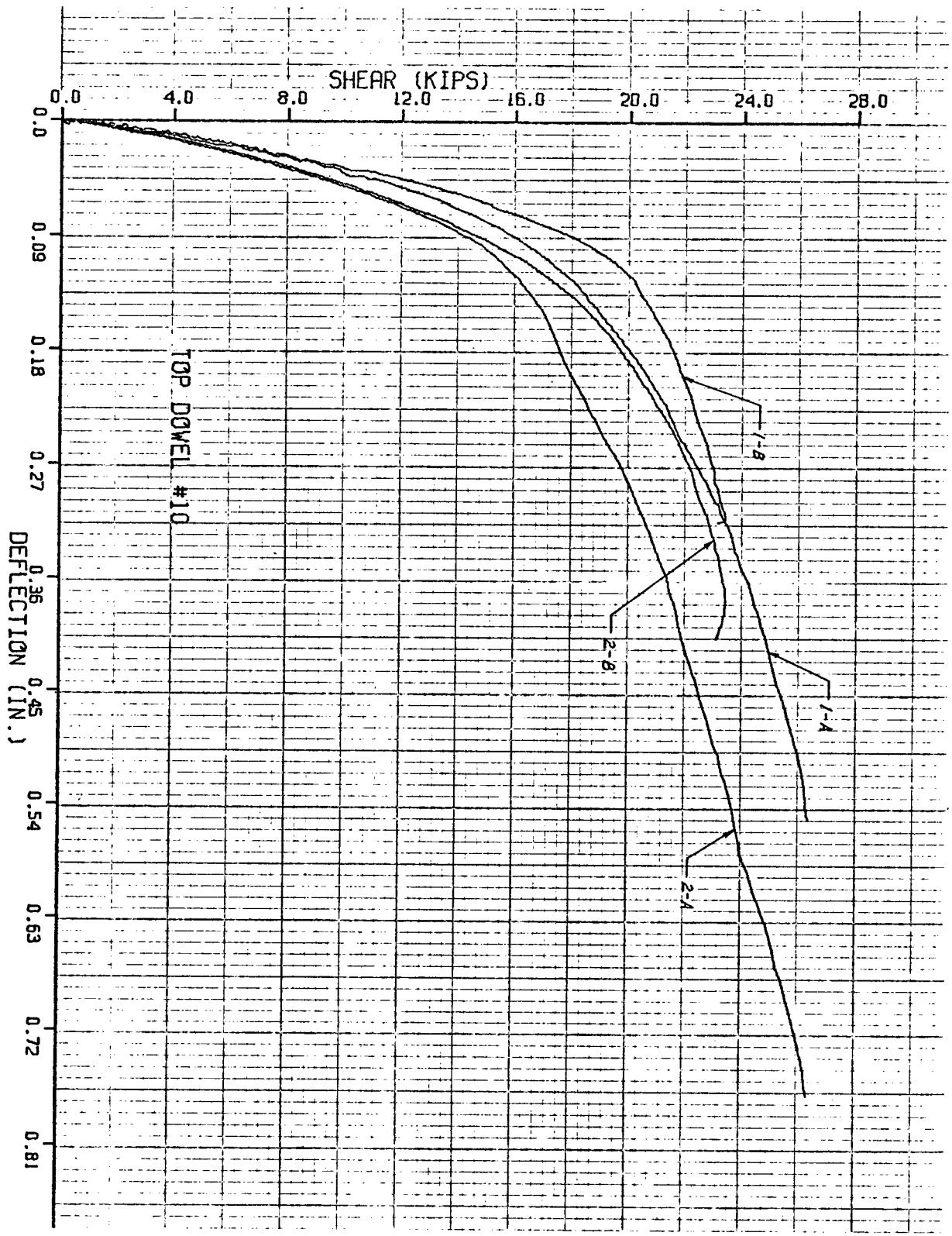
SHEAR (KIPS)
0.0
4.0
8.0
12.0
16.0
20.0
24.0
28.0
DEFLECTION (IN.)
0.0
0.09
0.18
0.27
0.36
0.45
0.54
0.63
0.72
0.81
TOP DOWEL #10
1-B
2-B
1-A
2-A

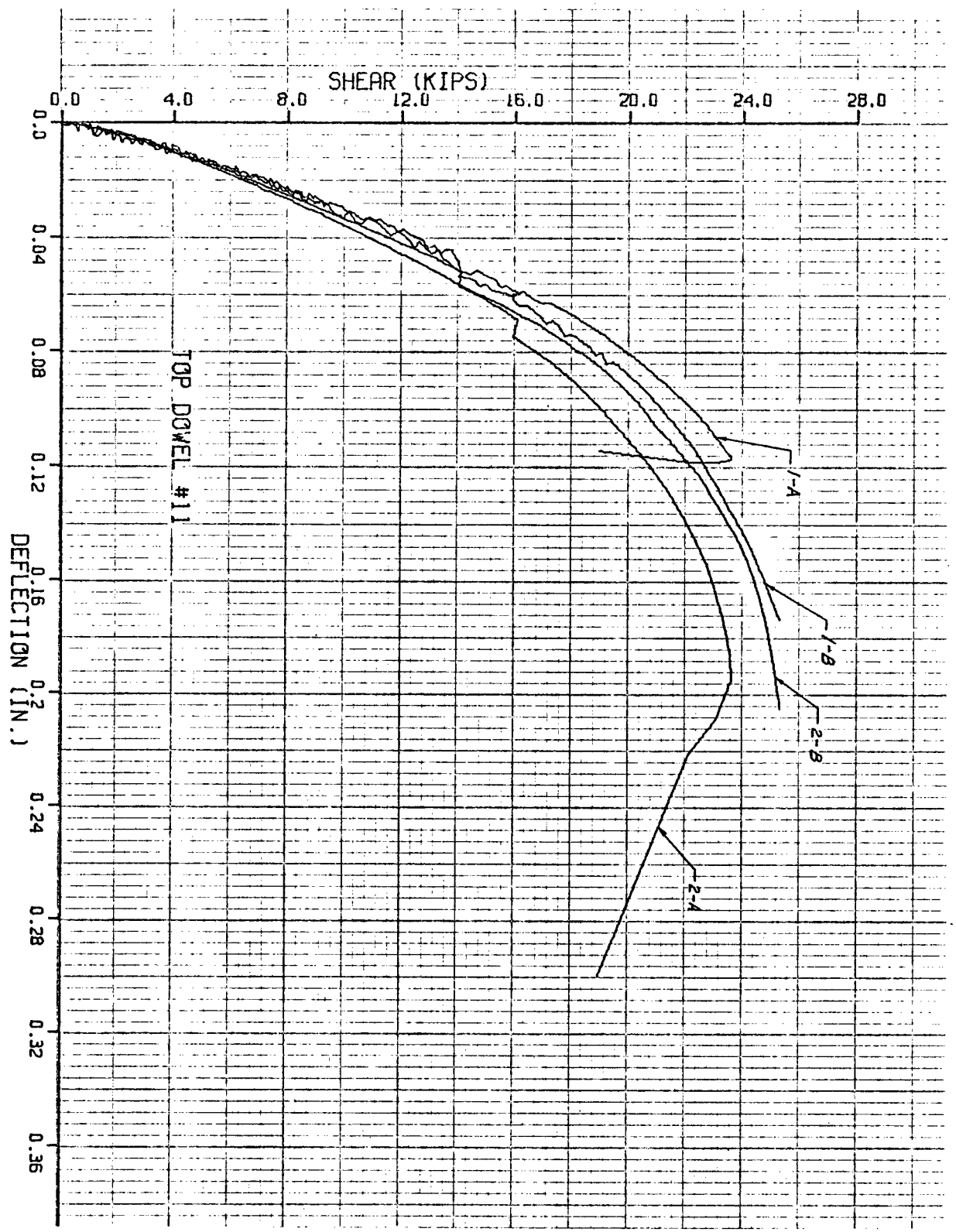
SHEAR (KIPS)
0.0
4.0
8.0
12.0
16.0
20.0
24.0
28.0
DEFLECTION (IN.)
0.0
0.04
0.08
0.12
0.16
0.2
0.24
0.28
0.32
0.36
TOP DOWEL #11
1-A
1-B
2-B
2-A